Pergamon

PII: S0301-9322(97)00005-0

Int. J. Multiphase Flow Vol. 22, Suppl., pp. 21–66, 1996

Printed in Great Britain
0301-9322/96 $15.00 + 0.00

EULERIAN TWO-PHASE FLOW THEORY APPLIED TO FLUIDIZATION

H. ENWALD[1], E. PEIRANO[2] and A.-E. ALMSTEDT[1]†

[1]Department of Thermo and Fluid Dynamics, [2]Department of Energy Conversion, Chalmers University of Technology, 412 96 Göteborg, Sweden

(Received 24 July 1995; in revised form 5 February 1997)

Abstract—A general classification of two-phase flows and a number of possible ways to formulate two-fluid models are discussed. The two-fluid model is adopted, and a general procedure to develop such a model is presented. The local instantaneous equations of mass and momentum are derived together with the corresponding jump conditions. Volume, time and ensemble averaging procedures are discussed, and averaged equations and jump conditions are derived using a general averaging operator. A Reynolds decomposition and weighting procedure is applied to obtain the final equations. The equations necessary to close the system, so-called closure laws, are discussed. The mechanisms contributing to the viscosity of both phases and mixture viscosity models are presented. The particle pressure is discussed, and some simple models based on the modulus of elasticity concept are given. The interfacial momentum transfer term is discussed in detail, and a study of common models of the drag function is presented. A discussion of turbulence models for the gas and particulate phases is included. A summary and critical assessment of published work on simulations of hydrodynamics in bubbling and circulating fluidized beds are also presented. © 1997 Elsevier Science Ltd.

Key Words: two-phase flow, fluidization, Eulerian, two-fluid model, turbulence

1. INTRODUCTION

1.1. Background

Two-phase flows are important in most industrial applications, examples being energy conversion, paper manufacturing, food manufacturing and medical applications. It is of great interest for the development of these applications to achieve a basic understanding of the complex flow situations that arise. Vast numbers of experiments have been carried out for different applications, a strategy that produces specific but expensive results. With modern computer technology, however, it is possible to numerically solve the partial differential equations describing multidimensional, time-dependent two-phase flow problems. It is thus interesting to develop the theoretical background to a higher level. Empirical models are needed to close the set of equations and, consequently, successful modelling is strongly dependent on experimental data.

Two-phase flow problems can be modelled in several ways. In some applications, e.g. film boiling (separated flow), the two phases can be modelled with the established equations for single-phase flows with a moving boundary between the phases. In practice, however, many flows are well mixed and, for such cases, this method cannot be used. In applications with well mixed phases, e.g. when the number of particles or droplets in the dispersed phase is large, averaging procedures are necessary to make the equations solvable. The most important averaging procedures are space average, time average and ensemble average.

The following sources are comprehensive publications on the derivation of basic two-phase flow equations and different averaging procedures: Ishii (1975), Delhaye and Achard (1977), Bouré and Delhaye (1982), Soo (1990), Drew and Lahey (1993) and He and Simonin (1994). These references are recommended as a complement to the present publication.

†Author to whom correspondence should be addressed.

1.2. Scope of this study

The purpose of this study is to provide insight for newcomers in the field of simulation of two-phase flows in fluidized beds. An attempt has been made to gather important models and findings from a wide range of different publications to give a rapid introduction to the available approaches to this physically and mathematically complex field.

This report describes the two-fluid model, derived with a general averaging procedure. The derivation of the local instantaneous mass and momentum equations is described in section 2. The methods of ensemble, time and space averaging are discussed briefly and these methods are applied to the local instantaneous equations in section 3 and appendix B. The closure laws, i.e. topological, constitutive and transfer laws, are discussed in detail in section 4. The models described in sections 2–4 will be referred to as traditional models. Section 5 describes a two-fluid model including turbulence of both phases. Section 6 presents a summary of work done by different research groups on the simulation of bubbling and circulating fluidized beds and gives a critical assessment of the methods used.

1.3. Classification of two-phase flows

The variety of possible two-phase flow problems is illustrated by the different classification methods suggested in the literature. A general classification is that of Ishii (1975), who divides two-phase flows into four groups depending on the constituents of the flow: gas–solid flows, gas–liquid flows, solid–liquid flows and flows of two immiscible liquids.

Ishii also makes a different classification depending on the topology of the flow, cf. table 1, which distinguishes between the three classes: separated flows, mixed flows and dispersed flows. Dispersed flows are studied in the present report. This class is in turn subdivided in terms of typical regimes, as shown in the table. Of these regimes, the present study treats the particulate flow. However, there are many different ways to characterize particulate flows as well. A classification by Kunii and Levenspiel (1991) based on the fluidization velocity and particle properties is shown in figure 1 for the specific field of fluidization. A number of other classifications for different types of two-phase flows can be found in the literature, e.g. Hewitt (1982).

1.4. Classification of two-phase flow models

There are many ways to model a two-phase flow problem using partial differential equations (PDEs), depending on the physical phenomena of interest and the nature of the problem. In this report, interest is focused on Eulerian three-dimensional models. Ishii (1975) divides these into the two categories of diffusion models and two-fluid models. A diffusion model is formulated by considering the mixture as a whole, and can be represented by one continuity equation, one momentum equation in each coordinate direction, one energy equation and one diffusion equation, to take into account the effect of concentration gradients. A two-fluid model, which is the model under consideration in the present work, consists of two continuity equations, two momentum equations in each coordinate direction and two energy equations. Additional closure laws are needed to close the set of equations, as described below.

1.5. Formulation of a two-fluid model

There are many ways, depending on the averaging procedure and the closure laws adopted, to formulate a two-fluid model. The general idea is to first formulate the integral balances for mass, momentum and energy for a fixed control volume containing both phases. This balance must be satisfied at any time and at any point in space, and thus reduces into two types of local equations, one being the local instantaneous equations for each phase and the other an expression of the local instantaneous jump conditions, i.e. the interactions between the phases at the interface. In principle, this set of equations could be solved by direct simulation, i.e. using a numerical mesh finer than the smallest length scales of the flow and a time step shorter than the time scales of the fastest fluctuations. This would require quite unrealistic computational times, however.

An alternative method would be to apply a Lagrangian approach for the particulate phase, although this would result in too large a number of equations for cases with many particles, i.e. for most practical applications. Recent attempts to use Lagrangian models are the work by Hoomans *et al.* (1996) who simulated a single rising bubble in a two-dimensional bubbling fluidized

bed, and Yonemura *et al.* (1995) who studied numerically the effects of the physical properties of the particles on the structure of particle clusters in circulating fluidized beds.

For the Eulerian approach, discussed in the present paper, the local instantaneous equations must be averaged in a suitable way, either in space, in time or as an ensemble. This allows a coarser mesh and a longer time step to be used in the numerical simulation, but, alas, introduces more unknowns than the number of equations into the system, and thus necessitates the inclusion of additional expressions to close the set of equations.

The closure laws are of three types: topological, constitutive and transfer laws, where the first type describes the spatial distribution of phase-specific quantities, the second type describes physical properties of the phases and the third type describes different interactions between the phases. As most of these expressions are empirical, experimental data are needed in order to develop and verify the laws. A general procedure for developing a two-fluid model is shown in figure 2. In the

Table 1. Different regimes for two-phase flows according to Ishii (1975)

Class	Typical regimes	Geometry	Configuration	Examples
Separated flows	Film flow		Liquid film in gas Gas film in liquid	Film cooling Film boiling
	Annular flow		Liquid core and gas film Gas core and liquid film	Film boiling Condensors
	Jet flow		Liquid jet in gas Gas jet in liquid	Atomization Jet condensor
Mixed or transitional flows	Slug or plug flow		Gas pocket in liquid	Sodium boiling in forced convection
	Bubbly annular flow		Gas bubbles in liquid Film with gas core	Evaporators with wall nucleation
	Droplet annular flow	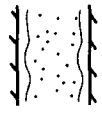	Gas core with droplets and liquid film	Steam generator
	Bubbly droplet annular flow		Gas core with droplets and liquid film with gas bubbles	Boiling nuclear reactor channel
Dispersed flows	Bubbly flow	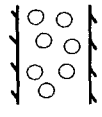	Gas bubbles in liquid	Chemical reactors
	Droplet flow		Liquid droplets in gas	Spray cooling
	Particulate flow	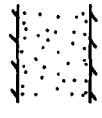	Solid particles in gas or liquid	Transportation of wheat

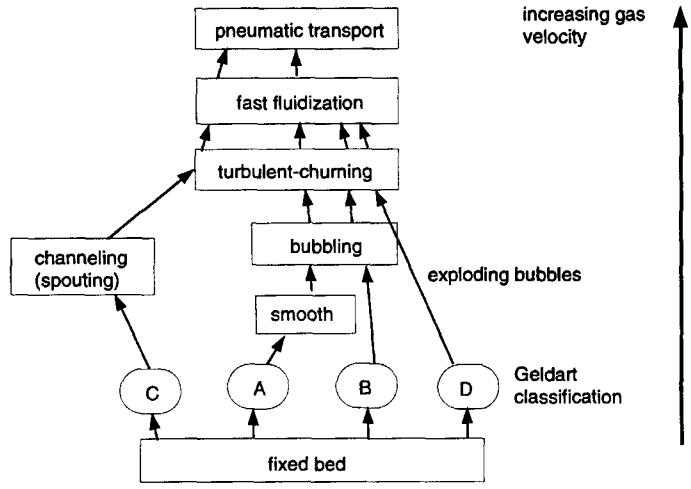

Figure 1. Gas–solid flow classification according to Kunii and Levenspiel (1991), based on the Geldart (1973) particle classification.

following, the averaging procedures are discussed in a general way, while the closure laws are discussed only for gas–particle flows.

2. LOCAL INSTANTANEOUS EQUATIONS

2.1. General equations

Several references can be found in which the local instantaneous equations are derived for both phases. The method used to derive the equations in this chapter was presented by Delhaye (1981) and by Bouré and Delhaye (1982).

Consider a general volume fixed in space (cf. figure 3) and shared by two phases with phase index k. The interface with the area between the phases $A_I(t)$ is moving with the velocity $\mathbf{u}_I$. When a vector or scalar variable ψ_k belonging to phase k is to be transported through the control volume using a coordinate system which is fixed (Eulerian approach), the following integral balance can be written

$$\sum_{k=1}^{2}\left(\frac{\mathrm{d}}{\mathrm{d}t}\int_{V_k(t)}\rho_k\psi_k\,\mathrm{d}V\right)=\int_{A_I(t)}\phi_I\,\mathrm{d}A+\sum_{k=1}^{2}\left(-\int_{A_k(t)}\rho_k\psi_k(\mathbf{u}_k\cdot\mathbf{n}_k)\mathrm{d}A+\int_{V_k(t)}\rho_k\phi_k\,\mathrm{d}V-\int_{A_k(t)}J_k\cdot\mathbf{n}_k\,\mathrm{d}A\right). \quad [1]$$

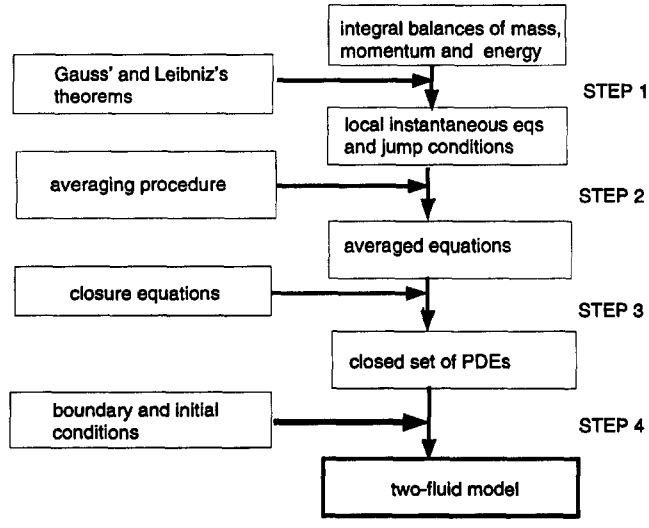

Figure 2. General procedure for formulating a two-fluid model.

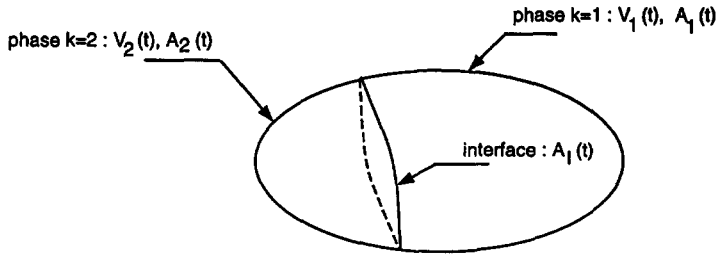

Figure 3. Fixed control volume containing two phases with a moving interface.

In this notation, $\mathbf{n}_k$ is the outwardly directed normal unit vector to the interface of the volume occupied by phase k, d/dt is the ordinary time derivative, $\mathbf{u}_k$ is the velocity of phase k, ρ_k is the density, ψ_k is the conserved quantity, J_k is the molecular flux, ϕ_k is the source term and ϕ_I is the interfacial source term. In [1], surface tension is not included in the formulation because these effects are negligible in gas–particle flows (the term involving surface tension would appear as a line integral over a curve which is the intersection of the fixed control volume and $A_I(t)$). A more complete formulation involving surface tension effects can be found in Delhaye (1974).

To continue the derivation, the velocity of a point on a geometric surface in space must be defined. Consider a surface defined by $\mathbf{r} = \mathbf{r}(x(\zeta, \eta, t), y(\zeta, \eta, t), z(\zeta, \eta, t))$. The velocity of the surface point, (ζ, η), is defined by

$$\mathbf{u}_I = \left(\frac{\partial \mathbf{r}}{\partial t}\right)_{\zeta,\eta = \text{const}}. \qquad [2]$$

The left-hand side of [1] can be transformed using Leibniz's theorem, [A4] in appendix A, into a volume integral and a surface integral which considers the movement of the interface. Furthermore, the convective term (the second term on the right-hand side) and the diffusion term (the last term on the right-hand side) can be rewritten as the sum of a volume and a surface integral using Gauss' theorem, [A1]–[A3] in appendix A. Thus,

$$\frac{\mathrm{d}}{\mathrm{d}t}\int_{V_k(t)} \rho_k\psi_k \,\mathrm{d}V = \int_{V_k(t)} \frac{\partial}{\partial t}(\rho_k\psi_k)\mathrm{d}V + \int_{A_I(t)} \rho_k\psi_k\mathbf{u}_I\cdot\mathbf{n}_k \,\mathrm{d}A, \qquad [3]$$

$$\int_{V_k(t)} \nabla\cdot(\rho_k\psi_k\mathbf{u}_k)\mathrm{d}V = \int_{A_k(t)} \rho_k\psi_k\mathbf{u}_k\cdot\mathbf{n}_k \,\mathrm{d}A + \int_{A_I(t)} \rho_k\psi_k\mathbf{u}_k\cdot\mathbf{n}_k \,\mathrm{d}A \qquad [4]$$

and

$$\int_{V_k(t)} \nabla\cdot J_k \,\mathrm{d}V = \int_{A_k(t)} J_k\cdot\mathbf{n}_k \,\mathrm{d}A + \int_{A_I(t)} J_k\cdot\mathbf{n}_k \,\mathrm{d}A. \qquad [5]$$

The surface integral over $A_k(t)$ in [3] vanishes because the speed of displacement of the boundary is zero as a consequence of the control volume being fixed.

Equation [1] can now be rewritten as one volume integral for the volumes occupied by the two phases and one surface integral which expresses the jump conditions across the interface

$$\sum_{k=1}^{2}\int_{V_k(t)}\left(\frac{\partial}{\partial t}(\rho_k\psi_k) + \nabla\cdot(\rho_k\psi_k\mathbf{u}_k) + \nabla\cdot J_k - \rho_k\phi_k\right)\mathrm{d}V - \int_{A_I(t)}\left(\sum_{k=1}^{2}(\dot{m}_k\psi_k + J_k\cdot\mathbf{n}_k) + \phi_I\right)\mathrm{d}A = 0. \qquad [6]$$

In the second integral of the above equation, $\dot{m}_k$ is the mass transfer per unit area of interface and unit time, defined as

$$\dot{m}_k = \rho_k(\mathbf{u}_k - \mathbf{u}_I)\cdot\mathbf{n}_k. \qquad [7]$$

Table 2. Values of ψ_k, J_k, ϕ_k and ϕ_I for the balance equations and jump conditions

Balance	ψ_k	J_k	ϕ_k	ϕ_I
Mass	1	0	0	0
Momentum	$\mathbf{U}_k$	$-\bar{\bar{T}}_k$	$\mathbf{b}$	0
Energy	E_k	$\mathbf{q}_k - \bar{\bar{T}}_k \cdot \mathbf{U}_k$	$\mathbf{b} \cdot \mathbf{U}_k$	0
Entropy	s_k	$\mathbf{q}_k/\theta_k$	Δ_k/ρ_k	Δ_I

Equation [6] must be satisfied for any $V_k(t)$ and $A_I(t)$. Thus, the local instantaneous equation is

$$\frac{\partial}{\partial t}(\rho_k \psi_k) + \nabla \cdot (\rho_k \psi_k \mathbf{u}_k) + \nabla \cdot J_k - \rho_k \phi_k = 0 \qquad [8]$$

and the local instantaneous jump condition is

$$\sum_{k=1}^{2} (\dot{m}_k \psi_k + J_k \cdot \mathbf{n}_k) = -\phi_I. \qquad [9]$$

The local instantaneous equation and the corresponding jump condition can be applied to the transport of mass, momentum, energy, entropy, chemical species and so on.

2.2. *Primary equations and jump conditions*

2.2.1. Introduction. The local instantaneous equations and the corresponding jump conditions for mass, momentum, energy and entropy are defined by table 2 and [8] and [9]. These sets of equations are called the primary equations and primary jump conditions, respectively. Secondary equations and secondary jump conditions, e.g. for the mechanical energy, can be derived from these equations if needed.

2.2.2. Conservation of mass.

$$\frac{\partial}{\partial t}(\rho_k) + \nabla \cdot (\rho_k \mathbf{u}_k) = 0, \qquad [10]$$

$$\sum_{k=1}^{2} \dot{m}_k = 0. \qquad [11]$$

2.2.3. Conservation of momentum.

$$\frac{\partial}{\partial t}(\rho_k \mathbf{u}_k) + \nabla \cdot (\rho_k \mathbf{u}_k \mathbf{u}_k) - \nabla \cdot \bar{\bar{T}}_k - \rho_k \mathbf{b} = 0, \qquad [12]$$

$$\sum_{k=1}^{2} (\dot{m}_k \mathbf{u}_k - \bar{\bar{T}}_k \cdot \mathbf{n}_k) = 0, \qquad [13]$$

where $\bar{\bar{T}}_k$ is the stress tensor and $\mathbf{b}$ is the body force (gravity).

3. GENERAL AVERAGING TECHNIQUE

3.1. *Averaging principles*

Modelling two-phase flows is a difficult task, both from a mathematical and a physical point of view. The mathematical difficulty lies in the formulation of the two-phase flow as two single phases with moving boundaries, while the physical difficulty lies in the modelling of the interaction between the phases at the interface. If the number of particles suspended in a gas flow is large, an averaging operator acting on the local instantaneous equations is needed (the alternative would be to solve one ordinary differential equation for each particle using a Lagrangian approach).

This section discusses the averaging methods of the local instantaneous equations and jump conditions. The use of averaging procedures in the two-phase flow theory has been extensively discussed in the literature. This chapter is based mainly on Ishii's book (1975), the publications of Delhaye and Achard (1977, 1978) and a publication by Delhaye (1981).

In the Eulerian approach, a given parameter, which can be a scalar, vector or tensor, is defined by the following equation: $f = f(\mathbf{r}, t)$. The parameter is thus studied at a fixed point in space, $\mathbf{r}$, at any time, t. At this point and time, either one of the phases may be present. To simplify the description, some kind of average is applied to the balance equations. The volume average is performed around the fixed point $\mathbf{r}$ at the time t, whereas the time average is performed at the point $\mathbf{r}$ over a time interval including the time t. The ensemble average is to be viewed as the statistical average of the parameter f_n at the point $\mathbf{r}$ and time t over a large number of experiments with the same initial and boundary conditions.

The volume average is defined as

$$\langle \ldots \rangle_v = \frac{1}{V} \int_V (\ldots) \mathrm{d}x \, \mathrm{d}y \, \mathrm{d}z. \qquad [14]$$

Whitaker (1969) gives the conditions under which the volume averaging procedure can be applied:

(characteristic dimension of phases)

$\ll$ (characteristic dimension of averaging volume)

$\ll$ (characteristic dimension of physical system).

The time averaging operator is defined by

$$\langle \ldots \rangle_t = \frac{1}{T} \int_{t - T/2}^{t + T/2} (\ldots) \mathrm{d}\tau. \qquad [16]$$

According to Delhaye and Achard (1977, 1978), the time interval chosen for the averaging must satisfy the following conditions:

(time scale of the turbulent fluctuations)

$\ll$ (time interval for averaging)

$\ll$ (time scale of the mean flow fluctuations).

For flows for which it is not possible to distinguish between the time scales of the turbulent fluctuations and the time scale of the mean flow, Delhaye and Achard (1977, 1978) introduce a double time-averaging operator.

The ensemble average, defined by

$$\langle \ldots \rangle_e = \int_\epsilon (\ldots) \mathrm{d}P(\mu), \qquad [18]$$

is the most general averaging process. In [18], $\mathrm{d}P(\mu)$ is the probability of observing process μ and ϵ is the set of all possible realizations, cf. Drew and Lahey (1993). A practical example of the meaning of the ensemble average is the averaging of a set of experiments in a fluidized bed starting with the same initial distribution of particles and the same initial gas and particle velocity distribution. There is thus no need to know the exact location of each particle nor the exact velocity fields in the beginning. In other words, the ensemble average is the statistical mean value of any parameter of interest at a given position and time over a number of experiments.

Both the time and spatial averages can be viewed as approximations of the ensemble average, which are valid provided the small and large time or space scales can be separated as described above. This is an application on a local scale of the ergodicity hypothesis, which states that if a flow is stationary and homogeneous, the ensemble, time and volume averages are equivalent.

The averaging procedure leads to a model describing two interpenetrating, continuous media. The averaging of the particulate phase is, on a larger scale, analogous to the averaging performed in the kinetic gas theory, when the averaging of the molecular motion leads to the description of the gas phase as a continuum, see also section 5.5. The single-phase equations of motion for a gas or liquid are regarded as local instantaneous equations, valid in a 'point' in space and time. A

'point' in this connection implies a space and time scale large enough to avoid the microscopic uncertainties in molecular motion but small enough to avoid macroscopic variations in the flow field. In analogy with this, the averaging of the particle motion in a disperse two-phase flow leads to averaged equations of motion for the continuous particulate phase, which in the same sense can be regarded as 'local instantaneous' equations, albeit on a larger scale.

The physical interpretation of the average, as a time, volume or ensemble average, may be important when formulating appropriate closure laws. However, the distinction between the different averages is not always obvious. For a fluidized bed, the three different types of averages may well be identical, provided the criteria above are fulfilled. For a fixed bed, however, where the particles do not move, a time average of the particle concentration at a given point in the bed will either give the value zero or one, cf. [19] and [20], while a volume average over a volume dV fulfilling the criteria above will give an appropriate value.

3.2. Derivation of the general averaged equations

The averaging methods presented above will be applied in the present section to transform the local instantaneous equations and jump conditions into averaged balance equations and corresponding averaged jump conditions. In so doing, the method presented by Drew (1983) is used.

As shown in [14], [15] and [18], the averaging operators for the volume, time and ensemble averages are formally similar. Thus, in the following, the general averaging operator $\langle \ldots \rangle$ denotes any of the specific operators defined above.

A few basic relations are first introduced. The phase indicator function, X_k, for phase k is a step function defined in the following way

$$X_k(\mathbf{r}, t) = \begin{cases} 1, & \text{if } \mathbf{r} \in k \\ 0, & \text{otherwise.} \end{cases} \qquad [19]$$

The average (ensemble, volume or time) of the phase indicator function is equivalent to the average occurrence of phase k

$$\alpha_k = \langle X_k \rangle, \qquad [20]$$

where

$$\sum_{k=1}^{2} \alpha_k = 1. \qquad [21]$$

In the following, the average occurrence of the gas phase, α_G, is referred to as the voidage.

The averaging procedure is assumed to have the following properties

$$\langle f + g \rangle = \langle f \rangle + \langle g \rangle, \qquad [22]$$

$$\langle \langle f \rangle g \rangle = \langle f \rangle \langle g \rangle, \qquad [23]$$

$$\langle \text{constant} \rangle = \text{constant}, \qquad [24]$$

$$\left\langle \frac{\partial f}{\partial t} \right\rangle = \frac{\partial \langle f \rangle}{\partial t}, \qquad [25]$$

$$\langle \nabla f \rangle = \nabla \langle f \rangle, \qquad [26]$$

$$\langle \nabla \cdot f \rangle = \nabla \cdot \langle f \rangle. \qquad [27]$$

Using the definition of the phase indicator, [19], together with [22]–[27] and the chain rule, the following relations can be derived

$$\frac{\partial \langle X_k f_k \rangle}{\partial t} = \left\langle \mathbf{X}_k \frac{\partial f_k}{\partial t} \right\rangle + \left\langle f_k \frac{\partial X_k}{\partial t} \right\rangle, \qquad [28]$$

$$\nabla\langle X_k f_k\rangle = \langle X_k \nabla f_k\rangle + \langle f_k \nabla X_k\rangle, \quad [29]$$

$$\nabla\cdot\langle X_k f_k\rangle = \langle X_k \nabla\cdot f_k\rangle + \langle f_k\cdot\nabla X_k\rangle. \quad [30]$$

Another fundamental relation is the following, which was derived by Drew (1983)

$$\frac{\partial X_k}{\partial t} + \mathbf{u}_I\cdot\nabla X_k = 0. \quad [31]$$

According to Drew and Lahey (1993), [31] can be interpreted as the material derivative of the phase indicator following the interface.

The first step in the averaging procedure is to multiply the local instantaneous equation, [8], by the phase indicator function and form the average of the resulting equation. With the aid of [28]–[31], the general form of the averaged balance equation is then obtained as

$$\frac{\partial}{\partial t}\langle X_k\rho_k\psi_k\rangle + \nabla\cdot\langle X_k\rho_k\psi_k\mathbf{u}_k\rangle + \nabla\cdot\langle X_k J_k\rangle - \langle X_k\rho_k\phi_k\rangle = \left\langle (\dot{m}_k\psi_k + J_k\cdot\mathbf{n}_k)\frac{\partial X_k}{\partial n}\right\rangle. \quad [32]$$

The right-hand side of the equation is the interfacial transport term. The gradient of the phase indicator function is expressed as $\nabla X_k = (\partial X_k/\partial n)\mathbf{n}_k$, where

$$\frac{\partial X_k}{\partial n} = -\delta_k. \quad [33]$$

Here, δ_k, is the Dirac's delta function associated with phase k. Thus, the gradient serves to sort out the mass and molecular fluxes at the interface. The Dirac delta function has the property

$$\int_{-\infty}^{+\infty} f(\xi)\delta(\xi - a)\mathrm{d}\xi = f(a) \quad [34]$$

and, thus, averaging the product of the absolute value of the gradient and the fluxes gives as the result the average contributory effect of the mass and molecular fluxes at the interfaces over the whole domain of integration.

The gradient of the phase indicator function is also used when transforming the local instantaneous jump condition [9], into an averaged jump condition

$$\sum_{k=1}^{2}\left\langle (\dot{m}_k\psi_k + J_k\cdot\mathbf{n}_k)\frac{\partial X_k}{\partial n}\right\rangle = -\left\langle \phi_I\frac{\partial X_k}{\partial n}\right\rangle. \quad [35]$$

In the following sections, the averaged balance equations for mass and momentum are presented together with the corresponding averaged jump conditions.

3.3. Averaged transport of mass and momentum

The specific balance equations of mass and momentum and the corresponding jump conditions are given by the general averaged balance equation [32], the general averaged jump condition, [35], and table 2. For a case in which there is no mass transfer between the phases, i.e. in which $\dot{m}_k = 0$, the following equations are obtained. Averaged continuity equation

$$\frac{\partial}{\partial t}\langle X_k\rho_k\rangle + \nabla\cdot\langle X_k\rho_k\mathbf{u}_k\rangle = 0. \quad [36]$$

With no mass transfer between the phases, the mass jump condition vanishes.

Averaged momentum equation with the body force equal to the gravitational acceleration

$$\frac{\partial}{\partial t}\langle X_k\rho_k\mathbf{u}_k\rangle + \nabla\cdot\langle X_k\rho_k\mathbf{u}_k\mathbf{u}_k\rangle - \nabla\cdot\langle X_k\bar{\bar{T}}_k\rangle - \langle X_k\rho_k\mathbf{g}\rangle = \langle -\bar{\bar{T}}_k\cdot\nabla X_k\rangle = \mathbf{M}_{kI}, \quad [37]$$

where $\mathbf{M}_{kI}$ is the interfacial momentum transfer.

Averaged momentum jump condition

$$\sum_{k=1}^{2} \langle -\bar{\bar{T}}_k \cdot \nabla X_k \rangle = \sum_{k=1}^{2} \mathbf{M}_{ki} = \mathbf{0} \Rightarrow \mathbf{M}_{1i} = -\mathbf{M}_{2i}. \quad [38]$$

All the terms on the left-hand side of the balance equations represent self-interacting quantities, while the terms remaining on the right-hand side are interfacial transfer terms, i.e. they represent interactions between the phases. As described in section 4.4 below, the transfer terms are modelled using empirical expressions, and the jump conditions place constraints on these.

3.4. Reynolds-decomposed and weighted averaged equations

3.4.1. Reynolds decomposition. The averaged equations presented above cannot be solved directly, as they contain averages of products of the dependent variables. To obtain a solvable set of equations, they must first be rewritten into expressions containing products of the averaged variables. This is done by employing the Reynolds decomposition and a weighting procedure to the variables before averaging, as demonstrated by Drew and Lahey (1993) for an ensemble-averaged two-fluid model and by Ishii (1975) for a time-averaged two-fluid model. Reynolds decomposition and time averaging are normally used in the field of single-phase turbulence modelling in order to separate the fluctuating components of the variables from the time-averaged variables, but, here, the main purpose of the decomposition and weighting is to separate the averages of products into products of averages. The phrase 'Reynolds decomposition' is used, *stricto sensu*, in connection with time averaging, but this terminology is used in the present case regardless of the type of averaging procedure employed. The procedure will result in extra terms in the equations, containing correlations of the fluctuating components. These extra terms are analogous to the Reynolds stress terms in the case of single-phase turbulence modelling.

Applying the Reynolds decomposition and the weighting procedure to a general variable, f, the following expression is obtained

$$f = \langle f \rangle^{W} + f', \quad [39]$$

where the first term on the right-hand side is a weighted mean value and the primed term is the deviation from this mean value. The weighting procedure is described in section 3.4.2.

3.4.2. Weighted averaged variables. Generally, the weighted mean value of a given scalar or vector or a tensor f is defined by

$$\langle f \rangle^{W} = \langle Wf \rangle / \langle W \rangle, \quad [40]$$

where W is an arbitrary weighting factor. However, before further discussing weighted mean values, some theorems and definitions must be given.

The weighted mean value should have all properties given by [22]–[27]. To separate the average of products into products of averages, two different weighting procedures are used. The variables are either weighted with the phase indicator function (phasic average) or with the phase indicator function times the density (mass-weighted average or Favre average)

$$\langle f \rangle^{X_k} = \langle X_k f \rangle / \langle X_k \rangle \quad [41]$$

or

$$\langle f \rangle^{X_k \rho_k} = \langle X_k \rho_k f \rangle / \langle X_k \rho_k \rangle. \quad [42]$$

The reason for introducing the mass-weighted average is to be able to split up the correlations between the fluctuating density and the other fluctuating variables. For convenience, the weighted variables and terms are summarized below.

The velocities are taken as mass-weighted averages: $\langle \mathbf{u}_k \rangle^{X_k \rho_k}$ and $\langle \mathbf{u}_k' \rangle^{X_k \rho_k}$, where in the following, the notation $\langle \mathbf{u}_k \rangle^{X_k \rho_k} = \mathbf{U}_k$ will be used. Note also that the average of the fluctuating velocity equals zero, $\langle \mathbf{u}_k' \rangle^{X_k \rho_k} = 0$.

The density of phase k is weighted using the phasic average

$$\langle \rho_k \rangle^{X_k} = \langle X_k \rho_k \rangle / \langle X_k \rangle = \langle X_k \rho_k \rangle / \alpha_k = \rho_k^{X_k}. \quad [43]$$

The stress tensor of phase k is weighted using the phasic average

$$\langle \bar{\bar{T}}_k \rangle^{X_k} = \bar{\bar{T}}_k^{X_k}. \quad [44]$$

The averages presented above are all averages of single variables. In contrast to this, the fluctuation stress tensor of phase k is the phasic average of products of the fluctuating velocity components, defined as

$$\bar{\bar{T}}_k^{\mathrm{Re}} = -\langle X_k \rho_k \mathbf{u}_k' \mathbf{u}_k' \rangle / \langle X_k \rangle = -\langle X_k \rho_k \mathbf{u}_k' \mathbf{u}_k' \rangle / \alpha_k. \quad [45]$$

3.4.3. Reynolds-decomposed and weighted averaged equations. The decomposed form of the balance equations can be derived by applying Reynolds decomposition and rewriting the averaged equations with the aid of the weighted variables. The full details of the derivation are given in appendix B. The continuity and momentum equations can be summarized as follows.

Continuity equation

$$\frac{\partial}{\partial t}(\alpha_k \rho_k^{X_k}) + \nabla \cdot (\alpha_k \rho_k^{X_k} \mathbf{U}_k) = 0. \quad [46]$$

Momentum equation

$$\frac{\partial}{\partial t}(\alpha_k \rho_k^{X_k} \mathbf{U}_k) + \nabla \cdot (\alpha_k \rho_k^{X_k} \mathbf{U}_k \mathbf{U}_k) = \nabla \cdot (\alpha_k (\bar{\bar{T}}_k^{X_k} + \bar{\bar{T}}_k^{\mathrm{Re}})) + \alpha_k \rho_k^{X_k} \mathbf{g} + \mathbf{M}_{k1}. \quad [47]$$

In the momentum equation, the interfacial momentum transfer to phase k is denoted in the following way

$$\mathbf{M}_{k1} = -\langle \bar{\bar{T}}_k \cdot \nabla X_k \rangle. \quad [48]$$

As mentioned above, the momentum transfer is modelled using empirical expressions, and the jump condition places a constraint on this term. This is described in section 4.4.

4. CLOSURE LAWS

4.1. Basic principles

The equations in this section are applicable regardless of the averaging method used for the basic balance equations, and the averaging symbols are generally left out. When choosing closure laws for a two-fluid model, some basic principles must be considered in order to close the problem successfully, as discussed by Drew and Lahey (1993), Arnold *et al.* (1990) and Truesdell and Toupin (1960). Four of these principles are:

- equipresence;
- well-posedness;
- frame indifference;
- fulfilment of the second law of thermodynamics.

Equipresence means that any variable described by a closure law should be a function of all the other variables unless the independence of any of them can be shown. Well-posedness means that the set of differential equations has a unique solution which is stable. Frame indifference means that the closure laws should not depend on the reference frame.

An entropy inequality can be obtained from [8], table 2 and the second law of thermodynamics. According to Ishii (1975), this inequality is used as a restriction on the constitutive laws to ensure that the second law of thermodynamics is fulfilled. The entropy inequality should always be fulfilled, but most models do not take this into consideration. Arnold *et al.* (1990) presented a method to test whether the closure laws in combination with the balance equations fulfil the second law of thermodynamics. The entropy source originates both from heat transfer and from viscous dissipation. In many cases, the entropy increase is negligible, particularly for cases without heat transfer, as the viscous contribution is often small. However, the need to investigate the second law of thermodynamics should not be underestimated, as a violation of this principle is a warning that the model is not physically sound.

4.2. Classification of closure laws

A set of averaged partial differential equations describing a two-phase flow problem needs extra equations to close the system. As mentioned in section 1.5, the closure laws are of three types: constitutive, transfer and topological laws. The constitutive laws relate physical properties using axioms and experimental data. The transfer laws are empirical equations that describe the interaction between the phases occurring at the interface. The topological laws are sometimes needed to describe the spatial distribution of a flow variable, e.g. for one-dimensional pipe flow models of two-phase mixtures in which the radial concentration or velocity distribution of one of the phases may be needed.

The different types of closure laws just mentioned are sometimes grouped together and simply referred to as constitutive laws. However, as stated by Bouré and Delhaye (1982), the division of the closure laws into the three types mentioned is more appropriate, as these types have different physical significance.

The key to accurate modelling lies to a large extent in the closure laws used. A considerable number of models has been developed for this purpose, but, keeping in mind the vast numbers of possible two-phase flow configurations, it may still be difficult to find suitable closure laws for a specific case. To limit the present study, only closure laws appropriate for gas–particle flows have been considered.

4.3. Constitutive laws

The constitutive laws specify how the physical parameters of a phase interact with each other, but do not describe the transport of mass, momentum or energy across the interface between the phases. The interfacial momentum transfer is described in section 4.4, while interfacial mass and energy transfer have been excluded from this study. For the particulate phase, there are two quite different ways of modelling such flow parameters as dynamic viscosity, bulk viscosity and particle pressure. One is to make empirical models based on the particle properties and the local voidage. These traditional models are relatively simple, and are thus easy to implement in a computer code. The traditional models will be discussed in the present section. The other way to model these properties is to use the so-called kinetic theory of granular flow, e.g. Jenkins and Savage (1983) and Savage and Jeffrey (1981). Generally, these kinds of models are more complex and time-consuming to solve, but many researchers believe that they are applicable for a wider range of problems. Models based on the kinetic theory of granular flow are discussed in section 5.

4.3.1. Viscous stress. The viscous stress of phase k of a two-phase mixture, $\bar{\bar{\tau}}_k$, enters into the momentum equations from the term $\nabla\cdot(\alpha_k \bar{\bar{T}}_k^{X_k})$ in [47], which is split up into a pressure term and a shear stress term as

$$\nabla\cdot(\alpha_k \bar{\bar{T}}_k^{X_k}) = \nabla\cdot(\alpha_k(-P_k\bar{\bar{I}} + \bar{\bar{\tau}}_k)) = -\nabla(\alpha_k P_k) + \nabla\cdot(\alpha_k \bar{\bar{\tau}}_k). \quad [49]$$

The physical phenomena in gas–particle flows giving rise to the viscous stress are not well understood, and the literature is inconsistent in the use of terms such as mixture viscosity, apparent viscosity, effective viscosity, suspension viscosity, etc.

When studying the literature, it is sometimes not fully clear whether an author refers to a stress in the gas phase, in the particulate phase or in the mixture as a whole. Furthermore, when discussing the particulate phase viscosity, μ_p, it is often uncertain whether or not the fluctuating stress tensor contribution has been included, i.e. the shear contribution of the tensor $\bar{\bar{T}}_k^{Re}$.

The stress tensor of both phases is often modelled using the Newtonian strain–stress relation

$$\bar{\bar{\tau}}_k = \xi_k(\nabla\cdot\mathbf{U}_k)\bar{\bar{I}} + 2\,\mu_k(\bar{\bar{S}}_k - \tfrac{1}{3}(\nabla\cdot\mathbf{U}_k)\bar{\bar{I}}), \quad [50]$$

where the strain-rate tensor is defined by

$$\bar{\bar{S}}_k = \tfrac{1}{2}(\nabla\mathbf{U}_k + (\nabla\mathbf{U}_k)^T). \quad [51]$$

Non-Newtonian properties of the particulate phase can be taken into account by modelling the particle viscosity as a function of the voidage, $\mu_p = \mu_p(\alpha_G)$, as will be discussed further in this section. The bulk viscosity of phase k, ξ_k, is commonly set to zero in both phases, in accordance with Stokes' assumption, e.g. Panton (1984). In practice, the reason for neglecting the bulk viscosity

is the lack of reliable measurement techniques, cf. Pritchett *et al.* (1978). However, it is possible to derive an expression for the bulk viscosity theoretically, using the kinetic theory of granular flow, cf. section 5.

To fully describe the stress in each phase, as required for a two-fluid model, expressions for the gas and particle viscosities are needed. The gas and particle viscosities are often set to a constant value for each of the phases or are neglected. At high particle concentrations, the particle viscosity is several orders of magnitude larger than the gas viscosity. As mentioned earlier, the particle viscosity may be modelled as a function of the voidage. However, the vast majority of the viscosity models available are for the mixture viscosity only. It is not obvious how the mixture viscosity is related to the phase viscosities, but one way is to assume a linear relationship and weight the viscosities as

$$\mu_{mix} = \alpha_G \mu_G + (1 - \alpha_G)\mu_p. \qquad [52]$$

The validity of this crude assumption has not been verified, but it offers a way of modelling the particle viscosity for dilute suspensions by inserting the gas viscosity and the mixture viscosity taken from one of the mixture viscosity models presented below.

Table 3 gives a brief summary of mechanisms suggested in the literature to contribute to the viscosity of the respective phases. Note that the reasoning is quite similar for both phases when explaining the kinetic and collisional effects, the main difference being the different scales used for the phases. Hwang and Shen (1989) suggest that the particle presence effect gives rise to a stress in the particulate phase only. Many of the ideas used to define the particulate phase viscosity are closely related to the kinetic theory of gases.

Table 3. Viscocity mechanisms in the gas and particulate phases

Effect	Gas phase	Particulate phase
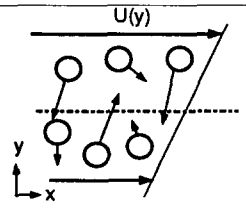 Kinetic effect	Random molecular motion across a plane and mean gas velocity gradient give rise to momentum transfer across the plane	Random particle motions across a plane and mean gas velocity gradient give rise to momentum transfer across the plane
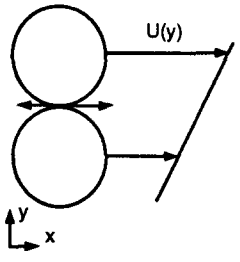 Collisional effect	Inter-molecular forces. When the average spacing of molecules is only a few times their diameter, attractive forces between the molecules become significant. Negligible in gases where the mean path is large, but important in liquids	Frictional inter-particle forces. May be very large when the solids concentration is high
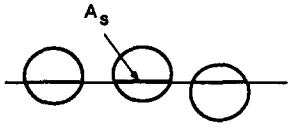 Particle presence effect	No contribution of this effect to the gas viscosity has been found in the literature	Shear stress acting on A_s due to the fluid force on the surface of the particles

The kinetic contributory effect to the viscosity of a gas can be understood by considering the gas on a molecular level, e.g. Panton (1984), pp. 142–145. The source of kinetic shear stress is the microscopic transport of momentum by random molecular motion across a plane, with different mean gas velocities on each side of the plane. The momentum difference that the gas molecules experience when they cross the plane is balanced by a shear stress acting on the plane. The kinetic contribution to the viscosity is, according to kinetic theory of gases, defined as the proportionality constant between the kinetic shear stress and the gradient of the mean gas velocity parallel to the plane with respect to a coordinate direction normal to the plane. A corresponding effect is present in the particulate phase, but on a larger scale, i.e. replacing the gas molecules with particles in the previous discussion.

The effect referred to as collisional viscosity is an effect of the tangential force arising from molecular interactions between nearby molecules, which can be likened to the frictional sliding that occurs between particles during a collision. In the gas phase, the molecules are at a mean distance such that the collisional effect is negligible as compared with the kinetic effect, but this effect dominates over the kinetic effect in a liquid, cf. Panton (1984). In the particulate phase, the collisional effect is the dominant contribution to the viscosity at high particle concentrations. The normal force arising from particle collisions is included in the collisional particle pressure term discussed in section 4.3.3.

Several workers discuss a viscosity effect arising from particles moving along the line of centres between the particles. This effect is referred to as the proximity effect in the present publication. The effect is related to the lubricating layers that exist between the particles in the gas-particle flow, i.e. to the viscous region in the gap between two nearby particles. In contrast to the effects discussed in table 3, the proximity effect is related to the mixture viscosity, and it is thus not included in the table. Theoretical models for the mixture viscosity based on this effect have been proposed by e.g. Einstein (1906, 1911) and by Frankel and Acrivos (1967), cf. below.

The first model presented for the mixture viscosity of dilute gas–particle flows with less than 3% volume concentration of particles was that of Einstein (1906, 1911), who proposed that

$$\mu_{\text{mix}} = \mu_{\text{G}}(1 + 2.5\alpha_{\text{p}} + O(\alpha_{\text{p}})), \quad \alpha_{\text{p}} \leqslant 0.03. \tag{53}$$

Another model for the mixture viscosity of dilute flows was presented independently by Brinkman (1952) and Roscoe (1952), and is given by the following equation:

$$\mu_{\text{mix}} = \mu_{\text{G}}(1 - \alpha_{\text{p}})^{-2.5}. \tag{54}$$

The mixture viscosities for dilute suspensions obtained from [53] and [54] are shown in figure 4.

In the limit of densely packed particles, e.g. in the dense part of a bubbling fluidized bed, a theoretical model based on the proximity effect was developed by Frankel and Acrivos (1967):

$$\mu_{\text{mix}} = \mu_{\text{G}} \frac{9}{8} \left(\frac{[\alpha_{\text{p}}/\alpha_{\text{p,max}}]^{1/3}}{1 - [\alpha_{\text{p}}/\alpha_{\text{p,max}}]^{1/3}} \right), \quad \alpha_{\text{p}}/\alpha_{\text{p,max}} \to 1, \tag{55}$$

where $\alpha_{\text{p,max}}$ is the maximum possible particle concentration.

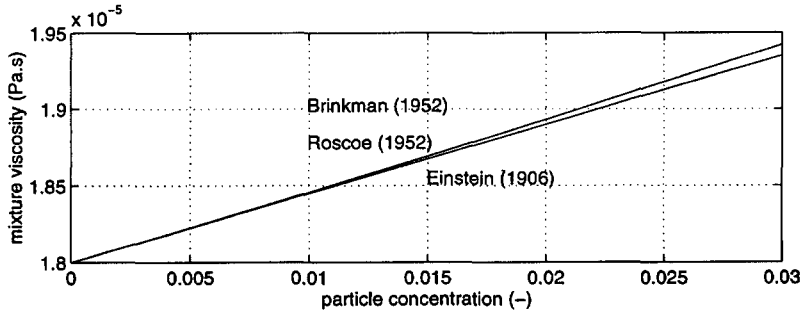

Figure 4. Mixture viscosities for dilute suspensions.

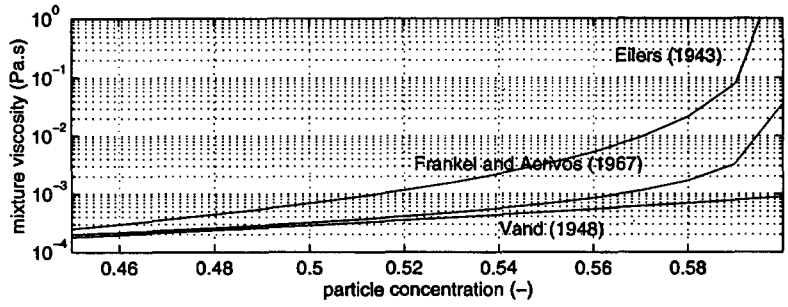

Figure 5. Mixture viscosities for dense suspensions.

Another theoretically based model applicable to high particle concentrations is presented by Vand (1948). In addition to the effect taken into account by Frankel and Acrivos, this model also includes the collisional effect of the particles. For spherical particles, the model can be stated as

$$\mu_{mix} = \mu_G \exp\left[\frac{2.5\alpha_p + 2.7\alpha_p^2}{1 - 0.609\alpha_p}\right]. \quad [56]$$

An empirical model for dense suspensions is that of Eilers (1943)

$$\mu_{mix} = \mu_G \frac{25}{16}\left(\frac{\alpha_p^2}{[1 - \alpha_p/\alpha_{p,max}]^2}\right). \quad [57]$$

The mixture viscosities for dense suspensions obtained from [55]–[57] are shown in figure 5.

Particle concentrations between the extremely dilute and extremely dense regions are commonly observed in many gas–particle flow applications, such as bubbling fluidization. A theoretical model that also covers the intermediate region was presented by Graham (1981)

$$\mu_{mix} = \mu_G\left(\frac{9}{4}\left[\frac{1}{1 + 0.5\psi}\right]\left[\frac{1}{\psi} - \frac{1}{1 + \psi} - \frac{1}{[1 + \psi]^2}\right] + 1 + 2.5\alpha_p\right), \quad [58]$$

where

$$\psi = \frac{1 - (\alpha_p/\alpha_{p,max})^{1/3}}{(\alpha_p/\alpha_{p,max})^{1/3}}. \quad [59]$$

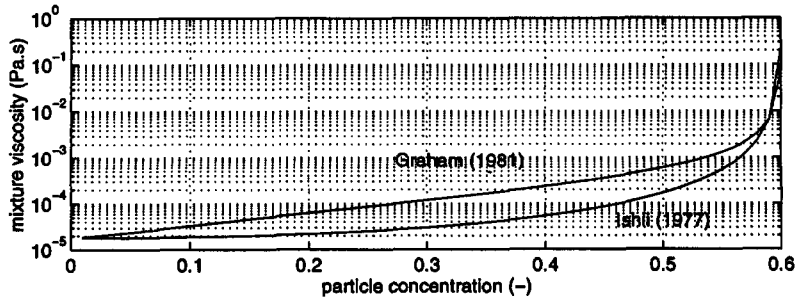

Figure 6. Mixture viscosities for the entire range of particle concentrations.

Table 4. Empirical constants for [64]

B_1	B_2	Source
−8.76	5.43	Gidaspow and Ettehadieh (1983)
−10.46	6.577	Ettehadieh *et al.* (1984)
−10.5	9.0	Gidaspow *et al.* (1989)

This model converges to Einstein's model, [53], in the limit of low particle concentrations, and to the Frankel and Acrivos model [55] in the limit of maximum particle packing.

Another model for the mixture viscosity covering the entire range of particle concentrations is that of Ishii (1977)

$$\mu_{mix} = \mu_G(1 - \alpha_p/\alpha_{p,max})^{-2.5\alpha_{p,max}(\mu_p + 0.4\mu_G)/(\mu_p + \mu_G)}. \quad [60]$$

Assuming the viscosity of the particulate phase to be considerably greater than that of the gas phase, [60] is simplified as

$$\mu_{mix} = \mu_G(1 - \alpha_p/\alpha_{p,max})^{-2.5\alpha_{p,max}}. \quad [61]$$

The mixture viscosities obtained from [58] and [61] are shown in figure 6.

4.3.2. Gas pressure. The gas pressure is set equal to the static pressure, $P_G = P$.

4.3.3. Particle pressure. The particle pressure is more difficult to interpret than the gas phase pressure. In the literature, there are two different ways of formulating expressions for the particle pressure. One is based on the kinetic theory of granular flow, which is an extension of the kinetic theory of dense gases, cf. section 5. Here, the alternative traditional approach based on the particle properties and the local voidage has been used, as described below.

The pressure in the particulate phase is considered as the sum of three effects, one corresponding to momentum transport caused by particle velocity fluctuation correlations, $P_{p,kin}$, one caused by particle interaction (collisions), $P_{p,coll}$, and one being a contribution from the gas phase pressure. The pressure gradient in the particulate phase is thus

$$\nabla(\alpha_p P_p) = \nabla(\alpha_p P_{p,kin}) + \nabla(\alpha_p P_{p,coll}) + \nabla(\alpha_p P_G). \quad [62]$$

The first term on the right-hand side of [62] is neglected in the traditional models. The second term of [62] is referred to as the particle collisional pressure gradient. A comprehensive discussion of the particle collisional pressure in fluidized beds is presented by Campbell and Wang (1991). The collisional component is the dominant effective pressure effect in the dense regions of a fluidized bed. This pressure transmits a force both by short-duration collisional impacts and by long-duration particle–particle contacts. Experimental results by Campbell and Wang show that the particle collisional pressure is highest if the bed is not fluidized and the particles rest on each other, i.e. when the long-duration contact force is high. As the gas flow increases towards the minimum fluidization velocity, the particle collisional pressure decreases as the drag force starts to dominate over the long-duration contact force. Increasing the gas velocity above the minimum fluidization velocity causes the particle collisional pressure to increase again, now as a result of an increasing frequency of the short-duration collisional impacts.

Table 5. Empirical constants for [65]

G_0	C	α^*	Source
1.0	600.0	0.376	Bouillard *et al.* (1989)
1.0	500.0	0.422	Gidaspow and Syamlal (1985)
1.0	20.0	0.62	Gidaspow and Ettehadieh (1983)

The gas pressure gradient enters into [62] as a 'buoyant' effect, i.e. if there is a gas pressure gradient through a collective of particles, it will exert a force on the particles, and, thus, the particle pressure gradient will be reduced or increased depending on the sign of the gas pressure gradient, in accordance with [62].

Several models for the particle collisional pressure-gradient term presented in the literature are based on the following formulation

$$\nabla(\alpha_p P_{p,coll}) = -G(\alpha_G)\nabla\alpha_G. \quad [63]$$

The effect of the particle collisional pressure-gradient term is to keep the particles apart so that the calculated particle concentration does not exceed the maximum concentration obtainable for a given sphericity and size distribution of the particles. This term is more often referred to as the particle–particle interaction force, and this terminology will be used in the following. The function $G(\alpha_G)$ can be thought of as a modulus of elasticity for the particulate phase, which must be modelled empirically.

An overview of different models for the modulus of elasticity is given by Massoudi *et al.* (1992). The empirical models of G compared here are of two types

$$G(\alpha_G) = 10^{B_1\alpha_G + B_2} \quad [64]$$

or

$$G(\alpha_G) = G_0 e^{-C(\alpha_G - \alpha^*)}. \quad [65]$$

Empirical values for the constants in [64] and [65] obtained by different investigators are listed in tables 4 and 5, respectively, and the results are plotted in figures 7 and 8.

As shown in figures 7 and 8, the results obtained from the different models of G differ widely. The formulation of G as a function of the voidage only may not fulfil the principle of equipresence for closure laws by Drew and Lahey (1993), mentioned in section 4.1, which could then partly explain the large discrepancies between the results. However, the main effect of the particle–particle interaction force is only to prevent the particulate phase from becoming too densely packed, and the large deviations between the different models for G may not significantly affect the time-averaged solutions for the concentration, velocity and pressure fields of the phases, although this remains to be investigated.

4.4. Transfer laws

4.4.1. Mechanisms of interfacial momentum transfer. Different mechanisms of interfacial momentum transfer have been discussed for one-dimensional two-fluid models by, e.g. Albråten (1982) and Andersson (1991). They investigated the importance of the different mechanisms by studying the dimensionless equations of motion and making comparisons with experimental results from fluidized beds. In the present work, a more general, three-dimensional formulation is used, cf. Ishii (1975) and Drew and Lahey (1993).

The term under consideration here is the interfacial momentum transfer term

$$\mathbf{M}_{kI} = -\langle \bar{\bar{T}}_k \cdot \nabla X_k \rangle \quad [66]$$

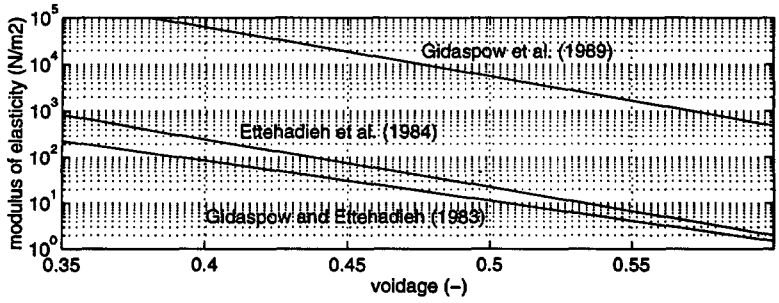

Figure 7. Modulus of elasticity obtained from [64].

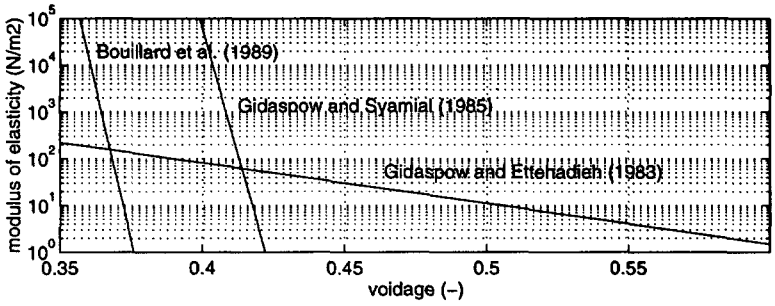

Figure 8. Modulus of elasticity obtained from [65].

from the Reynolds-decomposed and averaged momentum equation [47]. Neglecting the fluctuation stress term $\bar{\bar{T}}_k^{\mathrm{Re}}$, the right-hand side of [47] becomes

$$\begin{aligned}&\nabla\cdot(\alpha_k\bar{\bar{T}}_k)+\alpha_k\rho_k\mathbf{g}+\mathbf{M}_{k\mathrm{I}}\\&=-\alpha_k\nabla P-P\nabla\alpha_k-\nabla(\alpha_{\mathrm{p}}P_{\mathrm{p,coll}})+\nabla\cdot(\alpha_k\bar{\tau}_k)+\alpha_k\rho_k\mathbf{g}+\mathbf{M}_{k\mathrm{I}},\end{aligned}\tag{67}$$

where the stress tensor $\bar{\bar{T}}_k$ has been introduced as $\bar{\bar{T}}_k=-P_k\bar{\bar{I}}+\bar{\tau}_k$ and the gas pressure is set equal to the static pressure. The particle-particle interaction force, $-\nabla(\alpha_{\mathrm{p}}P_{\mathrm{p,coll}})$, is present only in the particulate phase equation. According to Drew and Lahey (1993), it has become customary to rewrite the interfacial momentum transfer, $\mathbf{M}_{k\mathrm{I}}$, in a form involving the interfacially averaged pressure and shear stress of phase k. To do this, the following definitions of the weighted averaged interfacial pressure and shear stress are introduced

$$\begin{aligned}P_{\mathrm{I}}&=\langle P\nabla X_k\cdot\mathbf{n}_k\rangle/\langle\nabla X_k\cdot\mathbf{n}_k\rangle,\\\bar{\tau}_{\mathrm{I}}&=\langle\bar{\tau}_k(\nabla X_k\cdot\mathbf{n}_k)\rangle/\langle\nabla X_k\cdot\mathbf{n}_k\rangle\end{aligned}\tag{68}$$

and $\mathbf{M}_{k\mathrm{I}}$ is rewritten as

$$\begin{aligned}\mathbf{M}_{k\mathrm{I}}&=-\langle\bar{\bar{T}}_k\cdot\nabla X_k\rangle\\&=\langle P\nabla X_k\rangle-\langle\bar{\tau}_k\cdot\nabla X_k\rangle\\&=P_{\mathrm{I}}\langle\nabla X_k\rangle-\bar{\tau}_{\mathrm{I}}\cdot\langle\nabla X_k\rangle-\langle\bar{\bar{T}}_{k\mathrm{I}}^{\mathrm{d}}\cdot\nabla X_k\rangle\\&=P_{\mathrm{I}}\nabla\alpha_k-\bar{\tau}_{\mathrm{I}}\cdot\nabla\alpha_k+\mathbf{M}_{k\mathrm{I}}^{\mathrm{d}}.\end{aligned}\tag{69}$$

Here, $\mathbf{M}_{k\mathrm{I}}^{\mathrm{d}}=-\langle\bar{\bar{T}}_{k\mathrm{I}}^{\mathrm{d}}\cdot\nabla X_k\rangle$ is a generalized drag force acting on phase k and

$$\bar{\bar{T}}_{k\mathrm{I}}^{\mathrm{d}}=-(P_k-P_{\mathrm{I}})\bar{\bar{I}}+(\bar{\tau}_k-\bar{\tau}_{\mathrm{I}})\tag{70}$$

is the generalized stress tensor associated with this drag.

A form of the jump condition for the interfacial momentum transfer is given by [38]. It can be shown that this jump condition is also applicable to the generalized drag. A summation of [69] over both phases gives

$$\sum_{k=1}^{2}\mathbf{M}_{k\mathrm{I}}=P_{\mathrm{I}}\sum_{k=1}^{2}\nabla\alpha_k-\bar{\tau}_{\mathrm{I}}\cdot\sum_{k=1}^{2}\nabla\alpha_k+\sum_{k=1}^{2}\mathbf{M}_{k\mathrm{I}}^{\mathrm{d}}.\tag{71}$$

The phasic relation, [21], can be differentiated to show that the first and second terms on the right-hand side of [71] are equal to zero. Using the momentum jump condition given by [38], the remaining part of [71] is the jump condition for the generalized drag

$$\sum_{k=1}^{2}\mathbf{M}_{k\mathrm{I}}^{\mathrm{d}}=0.\tag{72}$$

The right-hand side of the averaged momentum equation [67] can now be written as

$$-\alpha_k\nabla P-\nabla(\alpha_{\mathrm{p}}P_{\mathrm{p,coll}})+\nabla\cdot(\alpha_k\bar{\tau}_k)+\alpha_k\rho_k\mathbf{g}+\mathbf{M}_{k\mathrm{I}}^{\mathrm{d}}+(P_{\mathrm{I}}-P)\nabla\alpha_k-\bar{\tau}_{\mathrm{I}}\cdot\nabla\alpha_k,\tag{73}$$

where the last two terms are referred to as the interfacial pressure difference effect (or the concentration gradient effect) and the combined interfacial shear and void gradient effect, respectively. According to Albråten (1982) and Rathman (1981), the interfacial pressure difference effect is believed to be insignificant for the two-fluid model. According to Ishii and Mishima (1984), the combined interfacial shear and void gradient effect dominates over the generalized drag, $\mathbf{M}_{kI}^{d}$, for separated flows, but is generally ignored for dispersed flows, i.e. for the type of flow considered here. Thus, the right-hand side of [47] can be simplified as

$$-\alpha_k \nabla P - \nabla(\alpha_p P_{p,coll}) + \nabla\cdot(\alpha_k \bar{\bar{\tau}}_k) + \alpha_k \rho_k \mathbf{g} + \mathbf{M}_{kI}^{d}. \quad [74]$$

The generalized drag concept was originally conceived for gas liquid flows, e.g. Ishii and Mishima (1984), where the interfacial pressure difference effect and the combined interfacial shear and void gradient effect have a physical justification. However, the physical interpretation for gas–particle flows is less clear. For a dispersed flow, $\mathbf{M}_{kI}^{d}$ is the generalized drag force per unit of volume on a suspension of particles of mean diameter d_p, and it is normally divided as

$$\mathbf{M}_{pI}^{d} = n_p(\mathbf{F}_{dr} + \mathbf{F}_{tr} + \mathbf{F}_{am} + \mathbf{F}_{hi} + \mathbf{F}_{ot}), \quad [75]$$

where the forces in the brackets on the right-hand side of [75] are the forces acting on a single particle in a suspension and where n_p, the number of particles per unit volume, is defined as

$$n_p = 6(1 - \alpha_G)/\pi d_p^3. \quad [76]$$

The forces in [75] are discussed in the following subsections for the particulate phase only. The corresponding forces for the gas phase are obtained by changing signs in the particulate phase force expressions in accordance with the jump condition for the generalized drag [72].

4.4.2. Stationary drag force. The stationary drag models available in the literature are based either on correlations for the drag coefficient for one particle in a suspension, C_D, or on the pressure drop per unit length in a suspension.

The stationary drag force on a particle in a suspension can be defined either in terms of the relative superficial gas velocity or the relative interstitial velocity. It seems customary for researchers who base their models on the work of Richardson and Zaki (1954) to use the definition based on $\mathbf{U}_0 = \alpha_G(\mathbf{U}_G - \mathbf{U}_p)$, which is sometimes referred to as the apparent relative velocity, cf. Boemer *et al.* (1995). For researchers coming from other fields, for example boiling, the definition used is normally based on the relative interstitial velocity ($\mathbf{U}_r = \mathbf{U}_G - \mathbf{U}_p$).

The drag force acting on a single particle in a suspension can be written as

$$\mathbf{F}_{dr} = \tfrac{1}{2} C_D \rho_G |\mathbf{U}| \mathbf{U}(\pi d_p^2/4), \quad [77]$$

where $\mathbf{U}$ is either the apparent relative velocity or the relative interstitial velocity, depending on the velocity on which the drag coefficient C_D is based. The contributory effect of the stationary drag force to the generalized drag [75] is

$$n_p \mathbf{F}_{dr} = \frac{3}{4d_p}(1 - \alpha_G) C_D \rho_G |\mathbf{U}| \mathbf{U}. \quad [78]$$

For the pressure drop per unit of length in a suspension, Foscolo *et al.* (1983) showed that

$$n_p \mathbf{F}_{dr} = \alpha_G \nabla P. \quad [79]$$

To solve the averaged momentum equations numerically, the stationary drag force is usually written as

$$n_p F_{dr} = K \mathbf{U}_r, \quad [80]$$

where K is sometimes referred to as the drag function.

According to Di Felice (1994), the steady-state force balance applied to a particle in a suspension is

$$V_p \rho_p \mathbf{g} + \mathbf{F}_{dr} - V_p \nabla P = 0 \quad [81]$$

if there is no effect of particle collisions. The pressure gradient in a steady homogeneous suspension is equal to the buoyancy force exerted by the homogeneous mixture

$$\nabla P = \alpha_G \rho_G \mathbf{g} + (1 - \alpha_G)\rho_p \mathbf{g}. \quad [82]$$

This expression is sometimes referred to as the manometer formula, and it is obtained by adding the steady-state momentum equations of the two-fluid model, ignoring the viscous terms and the particle–particle interaction force. When [81] and [82] are combined, the drag force acting on a particle in a suspension can thus be expressed as

$$\mathbf{F}_{dr} = -\alpha_G V_p(\rho_p - \rho_G)\mathbf{g}. \quad [83]$$

This is the drag force included in the expression for the generalized drag, [75]. Wen and Yu (1966) formulated a slightly different expression for the stationary drag force, based on a steady-state force balance applied to a particle in a suspension similar to that of [81] but in which the pressure gradient was replaced by the buoyancy force, $\rho_G\mathbf{g}$, exerted by the gas phase only. Thus, the stationary drag force defined by Wen and Yu becomes

$$\mathbf{F}_K = -V_p(\rho_p - \rho_G)\mathbf{g} = \frac{1}{\alpha_G}\mathbf{F}_{dr}, \quad [84]$$

i.e. it differs by a factor α_G from the form of the stationary drag force included in [75]. In the work of Wen and Yu, it was shown that

$$|\mathbf{F}_K|/|\mathbf{F}_s| = C_{DK}/C_{Ds} = f(\alpha_G), \quad [85]$$

where the voidage function was taken as $f(\alpha_G) = \alpha_G^{-4.65}$, based on the work of Richardson and Zaki (1954).

To compute the drag function, K, the relation $C_D = \alpha_G C_{DK}$ obtained from [84] must be combined with [78], [80] and [85]. Employing the apparent relative velocity in [78], the following expression for the drag function, proposed by Gidaspow (1986), is obtained

$$K = \frac{3}{4d_p} C_{Ds}(1 - \alpha_G)\rho_G|\mathbf{U}_p - \mathbf{U}_G|\alpha_G^{-1.65}, \quad [86]$$

where the drag coefficient on a single sphere is given by Schiller and Naumann (1935)

$$C_{Ds} = \begin{cases} 24(1 + 0.15(\mathrm{Re})^{0.687})/\mathrm{Re} & \text{if } \mathrm{Re} < 1000 \\ 0.44 & \text{if } \mathrm{Re} > 1000 \end{cases} \quad [87]$$

and the Reynolds number is

$$\mathrm{Re} = \rho_G\alpha_G|\mathbf{U}_p - \mathbf{U}_G|d_p/\mu_G. \quad [88]$$

Reynolds numbers larger than 1000 are not often encountered in fluidized beds except at combinations of high pressure operation and large particles. The drag function correlation, [86], is valid only for dilute suspensions, with $\alpha_G > 0.8$. A summary of alternative correlations for the drag coefficient for a single sphere, C_{Ds}, is given in a book by Clift *et al.* (1978).

A different expression for the drag function for particulate flows, K, based on the relative interstitial velocity, was derived by Ishii and Zuber (1979). They introduced a Reynolds number based on the mixture viscosity, motivated by the fact that the presence of other particles makes a single particle see an increase in the resistance to its motion which appears as though it arises from an increased viscosity. Using a similarity hypothesis for the viscous regime, they derived the following expression

$$K = \frac{3}{4d_p} C_D(1 - \alpha_G)\rho_G|\mathbf{U}_p - \mathbf{U}_G|, \quad [89]$$

where the drag coefficient for a particle in the suspension is given as

$$C_D = 24(1 + 0.1(\mathrm{Re})^{0.75})/\mathrm{Re}, \quad [90]$$

and the Reynolds number is now defined as

$$\mathrm{Re} = \rho_G|\mathbf{U}_p - \mathbf{U}_G|d_p/\mu_{mix}. \quad [91]$$

The mixture viscosity is defined by [60], in which the maximum packing is $\alpha_{p,max} = 0.62$. The drag function correlation, [89], should be used with caution when α_p is close to its maximum value, $\alpha_{p,max}$,

because, in this limit, the mixture viscosity becomes infinite and the Reynolds number becomes zero, resulting in an infinite value of the drag function.

An alternative drag function correlation is that of Syamlal and O'Brien. This correlation has been used for both circulating and bubbling fluidized beds, cf. Syamlal and O'Brien (1988) and Syamlal and O'Brien (1989), respectively. The correlation is expressed as

$$K = \frac{3}{4d_p} C_D \rho_G \frac{1}{R_t^2} \alpha_G (1 - \alpha_G) |\mathbf{U}_p - \mathbf{U}_G|, \quad [92]$$

where R_t is the ratio of Richardson and Zaki, i.e. the ratio between the falling velocity of a suspension (superficial) and the terminal velocity of a single particle. Syamlal and O'Brien (1988) suggested a correlation for this ratio as a function of the Reynolds number based on the relative interstitial velocity and the voidage

$$2R_t = C_1(\alpha_G) - 0.06\mathrm{Re} + ((0.06\mathrm{Re})^2 + 0.12\mathrm{Re}(2C_2(\alpha_G) - C_1(\alpha_G)) + C_1^2(\alpha_G))^{0.5}, \quad [93]$$

where the functions $C_1(\alpha_G)$ and $C_2(\alpha_G)$ are given by

$$C_1(\alpha_G) = \alpha_G^{4.14} \quad \text{and} \quad C_2(\alpha_G) = \begin{cases} 0.8\alpha_G^{1.28} & \text{if } \alpha_G < 0.85 \\ \alpha_G^{2.65} & \text{if } \alpha_G > 0.85 \end{cases} \quad [94]$$

The drag coefficient in [92] is obtained from the correlation proposed by Dallavalle (1948)

$$C_D = \left(0.63 + 4.8\sqrt{\frac{R_t}{\mathrm{Re}}}\right)^2, \quad [95]$$

where

$$\mathrm{Re} = \rho_G |\mathbf{U}_p - \mathbf{U}_G| d_p / \mu_G. \quad [96]$$

Di Felice (1994) recently presented a correlation for a voidage function, $g(\alpha_G)$, which relates the stationary drag force for a particle in a suspension to the drag force on a single particle. This voidage function is related to the voidage function by Wen and Yu, [85], as

$$g(\alpha_G) = |\mathbf{F}_{dr}|/|\mathbf{F}_s| = C_D/C_{Ds} = \alpha_G f(\alpha_G). \quad [97]$$

Di Felice expresses the voidage function in the form $g(\alpha_G) = \alpha_G^{-\beta}$ which, in combination with [78], [80] and [97], gives an expression for the drag function, K. Employing the apparent relative velocity in [78], the following expression for the drag function is obtained

$$K = \frac{3}{4d_p} C_{Ds}(1 - \alpha_G)\rho_G |\mathbf{U}_p - \mathbf{U}_G| \alpha_G^{2-\beta}, \quad [98]$$

where the drag coefficient is given by Dallavalle (1948) as

$$C_{Ds} = \left(0.63 + 4.8\sqrt{\frac{1}{\mathrm{Re}}}\right)^2. \quad [99]$$

Di Felice showed that the exponent, β, is not a constant but depends on the Reynolds number as

$$\beta = 3.7 - 0.65 \exp(-(1.5 - \log(\mathrm{Re}))^2/2). \quad [100]$$

Figure 9 shows the different correlations based on C_D. The drag function is plotted as a function of the voidage for a relative interstitial velocity of 1.0 m/s, a sphericity of 1.0, a maximum particle volume concentration of 0.62, a mean particle diameter of 0.7 mm and a temperature of 293 K.

As shown in the figure, there is quite good agreement between the different correlations, with an exception for the correlation of Ishii and Zuber, [89]–[91], in the dense region. This deviation is a consequence of the mixture viscosity tending towards infinity.

One of the difficulties encountered in the freeboard region of circulating fluidized beds is the prediction of the clustering effect, cf. O'Brien and Syamlal (1993). The terminal velocity of a cluster

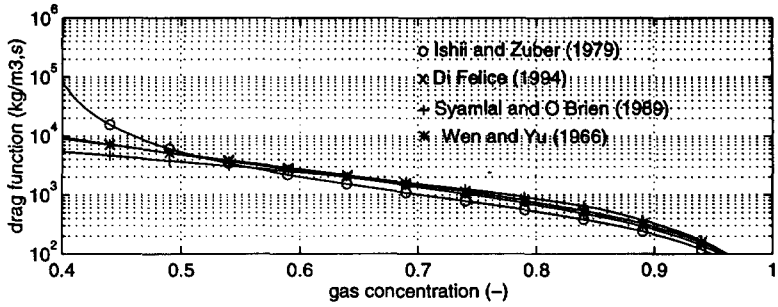

Figure 9. Comparison of the drag functions based on C_D.

exceeds the terminal velocity of a single particle. A correlation for the terminal velocity ratio taking into account the clustering effect is given by O'Brien and Syamlal (1993)

$$R_{clus} = R_t(1 + C_3(\alpha_G)\mathrm{Re}\,\alpha_G \exp(-0.005(\mathrm{Re} - 5)^2 - 90(\mathrm{Re} - 0.92)^2)), \quad [101]$$

where $C_3(\alpha_G)$ is defined by

$$C_3(\alpha_G) = \begin{cases} 250 & \text{if } G_p = 98 \text{ [kg/m}^2\text{, s]} \\ 1500 & \text{if } G_p = 147\text{[kg/m}^2\text{, s]} \end{cases} \quad [102]$$

and G_p is the particle recirculation mass flux. Replacing the velocity ratio, R_t with the velocity ratio corrected for cluster effects, R_{clus}, in the model by Syamlal and O'Brien, [92]–[94], yields a drag function that takes into account cluster effects.

Figure 10 shows the drag function, corrected for the clustering effect, for different mean particle diameters. This effect can be seen in the plots as a local minimum in the drag function in the voidage interval 0.7–0.95. As shown in the figure, the clustering effect decreases with increasing diameter. With the exception of the particle diameter, the flow parameters used in figure 10 are identical to the ones used for the correlations in figure 9.

A general correlation for the pressure drop per unit of length over a fixed bed was introduced by Ergun (1952), who proposed that

$$\frac{\Delta P}{L} = 150\frac{(1 - \alpha_{mf})^2}{\alpha_{mf}^3}\frac{\mu_G U_0}{(\phi d_p)^2} + 1.75\frac{(1 - \alpha_{mf})}{\alpha_{mf}^3}\frac{\rho_G U_0^2}{\phi d_p}. \quad [103]$$

Many researchers, e.g. Gidaspow (1994), assume the Ergun equation to be valid under fluidized conditions, for $\alpha_G < 0.8$, so that the equation can be rewritten as a drag function applicable to a two-fluid model. This expression of the drag function is obtained by combining the Ergun equation with [79], replacing the pressure gradient by $\Delta P/L$, and [80], as

$$K = 150\frac{(1 - \alpha_G)^2\mu_G}{\alpha_G(\phi d_p)^2} + 1.75\frac{(1 - \alpha_G)\rho_G|\mathbf{U}_p - \mathbf{U}_G|}{\phi d_p}. \quad [104]$$

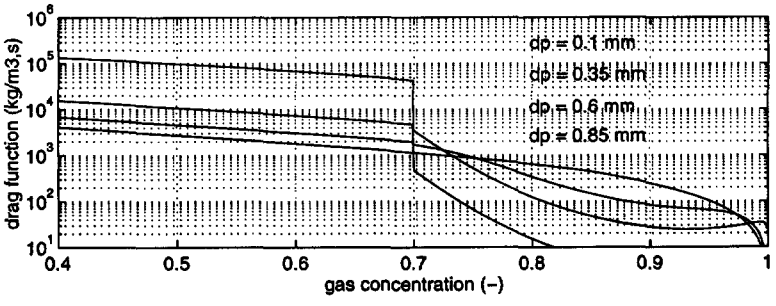

Figure 10. Drag function by Syamlal and O'Brien, [92]–[94], corrected for the clustering effect for different particle diameters with the aid of [101].

Gibilaro *et al.* (1985) introduced a correlation for the pressure drop per unit length for fluidized beds, covering the whole range of possible values for the voidage

$$\frac{\Delta P}{L} = \left(\frac{17.3}{\mathrm{Re}} + 0.336\right)\frac{\rho_G U_0^2}{d_p}(1 - \alpha_G)\alpha_G^{-4.8}. \quad [105]$$

Combining [105] with [79] and [80] and replacing the pressure gradient with $\Delta P/L$, the drag function becomes

$$K = \left(\frac{17.3}{\mathrm{Re}} + 0.336\right)\frac{\rho_G|\mathbf{U}_p - \mathbf{U}_G|}{d_p}(1 - \alpha_G)\alpha_G^{-1.8}, \quad [106]$$

where the Reynolds number is defined by [88].

Figure 11 shows the two correlations based on the pressure gradient for the same flow conditions as those in figure 9. The correlation given by Ergun shows quite good agreement with the correlations based on the drag coefficient, even though it was originally developed for a fixed bed, while the correlation of Gibilaro *et al.* gives the lowest values of all the drag function correlations, at least for the flow conditions chosen in the comparison. It should be noted that, of all the drag correlations included here, the Ergun correlation is the only one to take into account the particle sphericity.

4.4.3. Transverse forces. A particle moving in a fluid experiences a transverse force (sometimes referred to as lift force), if the flow is non-uniform (i.e. in the presence of a velocity gradient), if the particle is rotating or if the particle moves in the vicinity of a wall. Most investigations of transverse forces have been done for low Reynolds numbers ($\ll 1$) or for very large Reynolds numbers ($> 10^5$). Oesterlé (1994), however, made an investigation of these forces in the Reynolds number range of 1–1000, which is typical for gas–particle flows. The study does not take into account the presence of other particles, but the results can be applied if the particle diameter is very small in comparison with the distance between particles. The study shows that:

- the transverse forces are not negligible and tend to increase with increasing particle diameter;
- if there are no wall-particle collisions, the transverse force resulting from the velocity gradients is at least as important as the transverse force caused by the particle rotation;
- if there are wall-to-particle collisions, the transverse force caused by the velocity gradient decreases but is not negligible.

According to Drew and Lahey (1993), the transverse force resulting from the velocity gradients acting on the particles in a suspension per unit volume is given by

$$n_p\mathbf{F}_{tr} = -C_{tr}\rho_G(1 - \alpha_G)(\mathbf{U}_G - \mathbf{U}_p) \times (\nabla \times \mathbf{U}_G). \quad [107]$$

4.4.4. Added mass force. The added mass effect occurs when one phase accelerates in relation to the other. The accelerating phase must overcome the inertia of the mass that lies in its path. An

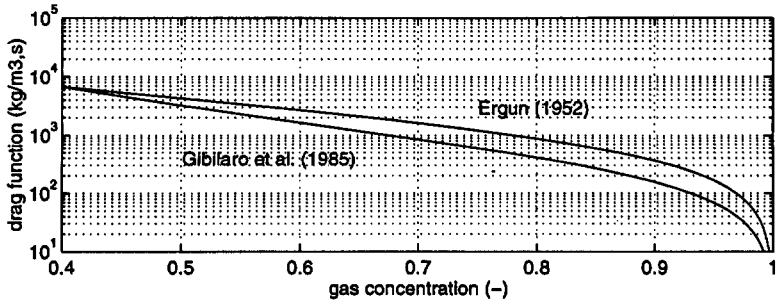

Figure 11. Comparison of drag functions based on the pressure gradient.

expression for the added mass force on the particles in a suspension per unit volume is given by Drew and Lahey (1993)

$$n_p \mathbf{F}_{am} = C_{am}(1 - \alpha_G)\rho_G\left(\frac{D_G \mathbf{U}_G}{Dt} - \frac{D_p \mathbf{U}_p}{Dt}\right). \quad [108]$$

The added mass coefficient, C_{am}, is, at least, a function of the voidage (cf. Zuber (1964) and Rathman (1981)).

Drew and Lahey (1990) stated that neither the added mass force, [108], nor the transverse force, [107], is frame-indifferent. Their sum is, however, for the case that both correction coefficients are equal, i.e. if $C_{tr} = C_{am}$, although in a personal communication with Drew and Lahey, Acrivos pointed out that a fundamental error had been made in the derivation and the conclusions were therefore modified to apply only to a fluid with small vorticity.

4.4.5. History force. The history force in two-phase flows comes from the acceleration of one phase relative to the other, and is a result of momentum being diffused through the boundary layer. The history force is sometimes also referred to as the Basset force. The history force acting on the particles in a suspension per unit of volume is

$$n_p \mathbf{F}_{hi} = \frac{9}{d_p}(1 - \alpha_G)\sqrt{\frac{\rho_G \mu_G}{\pi}} \int_0^t \frac{\mathbf{a}(\mathbf{r}, t)\mathrm{d}\tau}{\sqrt{t - \tau}}, \quad [109]$$

where the appropriate frame-indifferent acceleration, according to Drew and Lahey (1993), is given by

$$\mathbf{a}(\mathbf{r}, t) = \left(\frac{D_G \mathbf{U}_G}{Dt} - \frac{D_p \mathbf{U}_p}{Dt}\right) - (\mathbf{U}_G - \mathbf{U}_p) \times (\nabla \times \mathbf{U}_G). \quad [110]$$

4.4.6. Other forces. As shown by Arnold *et al.* (1989), forces additional to those mentioned above act on a sphere in an inviscid flow. Arnold *et al.* claim that it may be necessary to include some of these additional forces in order to fulfil the second law of thermodynamics, although they are usually ignored.

5. TURBULENT TWO-PHASE FLOWS

5.1. Background

For single-phase flow applications, turbulence is associated with the chaotic time-dependent multi-scale vortices occurring for flows with Reynolds numbers above a certain limit. The standard way of modelling turbulent single-phase flow is to derive a Reynolds decomposed and time-averaged form of the Navier–Stokes equations, cf. Hinze (1975). The equations differ from the laminar form by an extra stress term, the so-called Reynolds stress.

The meaning of turbulence is less established for gas–particle flows, and a short introduction is thus given below. The turbulence in the gas phase is similar to that of single-phase flows, although the generation and dissipation mechanisms may differ, as these are influenced by the presence of particles. Turbulence in the particulate phase can physically be understood as the particle velocity fluctuations caused by collisions between particles and interactions with the gas phase.

A description of turbulence models for the gas and particulate phases is presented in this section. The section starts with the introduction of a formulation of the transport equations (continuity and momentum), which is an alternative to the traditional formulation presented in section 3. This alternative formulation, derived by He and Simonin (1994), gives an explicit formulation for the interfacial momentum transfer using a Lagrangian approach, but it also introduces the need for new closure laws.

5.2. Transport equations

An expression for the interfacial momentum transfer for the particulate phase, $\mathbf{M}_{pI}$, can be obtained from the equation of motion of a single sphere in an infinite fluid, cf. He and Simonin

(1994). The equation of motion of a single sphere, moving in an unsteady non-uniform incompressible fluid, was proposed by Gatignol (1983) and Maxey and Riley (1983) for the case of a low particle Reynolds number, $\mathrm{Re} = \rho_G d_p |\mathbf{u}_p - \mathbf{u}_G|/\mu_G < 1$. They also made the assumptions that the gas flow characteristics vary slowly on the scale of a particle and that the size of the sphere is small compared with the smallest length scale of the gas flow. In most gas–particle flows characteristic for fluidization, the Reynolds numbers are in the range of 1–1000 for particles diameters in the range of 10^{-4}–10^{-3} m, cf. Oesterlé (1994). The equation of motion of a single sphere can be generalized in the case of compressible flows at higher Reynolds numbers, by

$$\rho_p \frac{\pi d_p^3}{6} \frac{\mathrm{d}\mathbf{u}_p}{\mathrm{d}t} = \frac{1}{2} \rho_G C_{Ds} \frac{\pi d_p^2}{4} |\tilde{\mathbf{u}}_G - \mathbf{u}_p| (\tilde{\mathbf{u}}_G - \mathbf{u}_p) + \frac{1}{2} \rho_G \frac{\pi d_p^3}{6} \Delta_A \frac{\mathrm{d}}{\mathrm{d}t} (\tilde{\mathbf{u}}_G - \mathbf{u}_p)$$

$$+ \frac{3 d_p^2}{2} \sqrt{\pi \rho_G \mu_G} \Delta_H \int_0^t \frac{\mathrm{d}}{\mathrm{d}\tau} (\tilde{\mathbf{u}}_G - \mathbf{u}_P) \frac{\mathrm{d}\tau}{\sqrt{t - \tau}} - \frac{\pi d_p^3}{6} \nabla \tilde{p} + \rho_p \frac{\pi d_p^3}{6} \mathbf{g}, \qquad [111]$$

where $\tilde{\mathbf{u}}_G$ and $\tilde{p}$ are the undisturbed gas velocity and pressure at the particle location, respectively, i.e. the velocity and pressure of the gas phase if the particle were not present. The terms on the right-hand side are identified as the stationary drag, the added mass force, the history force, the pressure gradient and the gravity force. Different correlations for the drag coefficient for a single sphere in an infinite fluid, C_{Ds}, and for the correction coefficients for the added mass and the history forces, Δ_A and Δ_H, can be found in the book by Clift *et al.* (1978).

It can be shown that the history force is negligible for gas–particle flows, provided that $\rho_G/\rho_p < 0.002$ and $d_p > 1$ μm, cf. Vojir and Michaelides (1994) and Liang and Michaelides (1992). Liang and Michaelides also concluded that the added mass effect can be neglected because the added mass term is proportional to the density ratio. It is generally assumed that these conclusions can be extended to a single particle in a suspension. Equation [111] can then be expressed in the following Eulerian form

$$\frac{\partial}{\partial t} (\rho_p \mathbf{u}_p) + \nabla \cdot (\rho_p \mathbf{u}_p \mathbf{u}_p) = \frac{\rho_p}{\tau_{Gp}^x} (\tilde{\mathbf{u}}_G - \mathbf{u}_p) - \nabla \tilde{p} + \rho_p \mathbf{g} + \mathbf{f}_c, \qquad [112]$$

where the particle relaxation time, τ_{Gp}^x, is

$$\frac{1}{\tau_{Gp}^x} = \frac{3}{4 d_p} \frac{\rho_G}{\rho_p} C_D |\mathbf{u}_p - \tilde{\mathbf{u}}_G| \qquad [113]$$

and $\mathbf{f}_c$ represents the force exerted by other particles during collisions. The particle relaxation time is a characteristic time for the entrainment of particles by the surrounding gas. Multiplying [112] by X_p and applying the averaging operator in combination with a Reynolds decomposition including the pressure term, $\tilde{p} = P + p'$, an averaged form of the particulate phase momentum equation is obtained

$$\frac{\partial}{\partial t} (\alpha_p \rho_p \mathbf{U}_p) + \nabla \cdot (\alpha_p \rho_p \mathbf{U}_p \mathbf{U}_p) = -\alpha_p \nabla P$$

$$+ \nabla \cdot (\alpha_p \bar{\bar{\tau}}_p^{X_p} + \alpha_p \bar{\bar{T}}_p^{Re}) + \alpha_p \rho_p \mathbf{g} + \mathbf{M}_{pI}', \qquad [114]$$

where the interfacial momentum term is given by

$$\mathbf{M}_{pI}' = -\frac{\alpha_p \rho_p}{\langle \tau_{Gp}^x \rangle^{X_p \rho_p}} \mathbf{U}_{rel} - \alpha_p \langle \nabla_p' \rangle^{X_p}. \qquad [115]$$

The collisional stress term, $\alpha_p \bar{\bar{\tau}}_p^{X_p}$, enters [114] from the average $\langle X_p \mathbf{f}_c \rangle$. The relative velocity is defined by

$$\mathbf{U}_{rel} = \mathbf{U}_p - \mathbf{U}_G - \langle \mathbf{u}_G' \rangle^{X_p \rho_p}, \qquad [116]$$

where $\langle \mathbf{u}_G' \rangle^{X_p \rho_p}$ is the drift velocity (cf. section 5.3). The drift velocity represents the correlation between the gas phase fluctuating velocity and the spatial distribution of the particles. According to Simonin (1990), this velocity represents the dispersion of the particles by the large turbulent scales of the gas phase.

It can be shown that this formulation is equivalent to the formulation of [47], obtained from the traditional approach, provided that the interfacial momentum transfer, $\mathbf{M}_{pI}$, is given by

$$\mathbf{M}_{pI} = -\frac{\alpha_p \rho_p}{\langle \tau_{Gp}^{X} \rangle^{X_p \rho_p}} \mathbf{U}_{rel} + \langle \tilde{p} \nabla X_G \rangle. \quad [117]$$

Neglecting the terms involving correlations of the pressure fluctuations, cf. Bel Fdhila and Simonin (1992), the momentum equations for both phases can be rewritten in the general form

$$\frac{\partial}{\partial t}(\alpha_k \rho_k \mathbf{U}_k) + \nabla \cdot (\alpha_k \rho_k \mathbf{U}_k \mathbf{U}_k) = -\alpha_k \nabla P + \nabla \cdot (\alpha_k \bar{\bar{\tau}}_k^{X_k} + \alpha_k \bar{\bar{T}}_k^{Re}) + \alpha_k \rho_k \mathbf{g} + \mathbf{M}'_{kI}, \quad [118]$$

where the interfacial momentum transfer, $M'_{pI} = -\mathbf{M}'_{GI}$, is given by $K(\mathbf{U}_G - \mathbf{U}_p)$ if the drift velocity is neglected. Thus, neglecting the drift velocity, the interfacial momentum transfer $\mathbf{M}'_{kI}$ equals the generalized drag $\mathbf{M}_{kI}^{d}$ of [74]. A detailed discussion of the approach presented in this section is given by Peirano (1996).

To close the momentum equations, models for the collisional and kinetic terms, $(\alpha_k \bar{\bar{\tau}}_k^{X_k} + \alpha_k \bar{\bar{T}}_k^{Re})$, as well as for the drift velocity are required.

5.3. *Drift velocity*

A model of the drift velocity, proposed by Deutsch and Simonin (1991), is expressed as

$$\langle \mathbf{u}'_G \rangle^{X_p \rho_p} = D_{Gp}^{t} \left(\frac{1}{\alpha_G} \nabla \alpha_G - \frac{1}{\alpha_p} \nabla \alpha_p \right), \quad [119]$$

with the assumption that the particles are suspended in homogeneous isotropic turbulence of the gas phase. The dispersion coefficient, D_{Gp}^{t}, is modelled as $\tau_{Gp}^{t} k_{Gp}/3$, where τ_{Gp}^{t} is the interaction time between particle motion and gas phase fluctuations defined in connection with [132], and k_{Gp} is the gas–particle covariance, defined in connection with [138]. If the turbulence is non-isotropic, the dispersion coefficient must be substituted with a tensor, cf. Deutsch and Simonin (1991).

More advanced models for the drift velocity can be derived, for example with the Lagrangian history direct interaction approximation, cf. Reeks (1992, 1993), with a fluid-particle joint probability density function (PDF) and the Langevin equation, cf. Simonin (1995), or with asymptotic solutions, cf. Koch (1990). The model based on the fluid–particle joint PDF gives a general transport equation for the drift velocity, whereas the model of Koch provides an algebraic expression with restrictions on the particle Reynolds number and the Stokes number. These models are not presented here, but an introduction to them is given by Peirano and Leckner (1997).

5.4. *Turbulence models for the gas phase*

A turbulence model for the gas phase of dilute suspensions was developed by Simonin and Viollet (1990). The model is a modified k–ϵ model with additional terms taking into account the interfacial turbulent momentum transfer. This model was later applied to a bubbling fluidized bed by Balzer *et al.* (1995).

The Reynolds stress tensor of the gas phase, $\bar{\bar{T}}_G^{Re}$, defined by [45], is modelled using a standard Boussinesq approximation

$$\bar{\bar{T}}_G^{Re} = -\rho_G \langle \mathbf{u}'_G \mathbf{u}'_G \rangle^{X_G \rho_G} = -\tfrac{2}{3} \rho_G k_G \bar{\bar{I}} + 2\mu_G^{t} (\bar{\bar{S}}_G - \tfrac{1}{3} (\nabla \cdot \mathbf{U}_G) \bar{\bar{I}}). \quad [120]$$

The dynamic turbulent viscosity of the gas phase, μ_G^{t}, is defined by $\mu_G^{t} = 2\rho_G k_G \tau_G^{t}/3$, and the time scale of the large eddies, τ_G^{t}, by $\tau_G^{t} = \frac{3}{2} C_\mu k_G/\epsilon_G$, cf. Simonin (1995). Furthermore, the turbulent kinetic energy in the gas phase, k_G, is modelled by the following transport equation

$$\frac{\partial}{\partial t}(\alpha_G \rho_G k_G) + \nabla \cdot (\alpha_G \rho_G k_G \mathbf{U}_G) = \nabla \cdot \left(\alpha_G \frac{\mu_G^{t}}{\sigma_k} \nabla k_G \right) - \alpha_G \rho_G \langle \mathbf{u}'_G \mathbf{u}'_G \rangle^{X_G \rho_G} \nabla \mathbf{U}_G - \alpha_G \rho_G \epsilon_G + \Pi_{k_G}, \quad [121]$$

where the interaction term, Π_{k_G}, is defined as

$$\Pi_{k_G} = \frac{\alpha_G \rho_G}{\tau^x_{Gp}} (-2k_G + k_{Gp} + \langle \mathbf{u}_G \rangle^{X_p \rho_p} \cdot \mathbf{U}_{rel}) \quad [122]$$

and the relative velocity, $\mathbf{U}_{rel}$, is defined by [116]. Finally, the differential equation for the dissipation of turbulent kinetic energy, ϵ_G, is given by

$$\frac{\partial}{\partial t}(\alpha_G \rho_G \epsilon_G) + \nabla \cdot (\alpha_G \rho_G \epsilon_G \mathbf{U}_G) = \nabla \cdot \left(\alpha_G \frac{\mu^t_G}{\sigma_\epsilon} \nabla \epsilon_G \right)$$

$$- \alpha_G \rho_G \frac{\epsilon_G}{k_G} (C_{\epsilon 1} \langle \mathbf{u}'_G \mathbf{u}'_G \rangle^{X_G \rho_G} \nabla \mathbf{U}_G + C_{\epsilon 2} \epsilon_G) + \Pi_{\epsilon_G}, \quad [123]$$

where the interaction term, Π_{ϵ_G}, is defined by

$$\Pi_{\epsilon_G} = C_{\epsilon 3} \frac{\epsilon_G}{k_G} \Pi_{k_G}. \quad [124]$$

The constants used in the k_G–ϵ_G model are chosen as $C_\mu = 0.09$, $\sigma_k = 1.0$, $\sigma_\epsilon = 1.3$, $C_{\epsilon 1} = 1.44$, $C_{\epsilon 2} = 1.92$ and $C_{\epsilon 3} = 1.2$. All these constants except $C_{\epsilon 3}$ have standard, single-phase flow turbulence values. The constant $C_{\epsilon 3}$ is included in the gas-particle interaction term, Π_{ϵ_G}, of the ϵ_G equation and has been determined empirically from turbulent gas–particle jet flows, cf. Elghobashi and Abou-Arab (1983).

It is reasonable to assume that the values of C_μ, $C_{\epsilon 1}$, $C_{\epsilon 2}$, $C_{\epsilon 3}$ should depend on the type of particles and the type of gas flow. Squire and Eaton (1994) investigated the values of $C_{\epsilon 2}$ and $C_{\epsilon 3}$ for homogeneous isotropic turbulence interacting with particles by comparing the solution of the k_G–ϵ_G model with direct numerical simulation (DNS) data. They showed that these two constants are functions of, at least, the Stokes number, τ^x_{Gp}/τ^t_G, and the loading, $X_{Gp} = \alpha_p \rho_p / \alpha_G \rho_G$, and that their order of magnitude can vary significantly for small Stokes numbers, i.e. for small particles affected by large eddies. The value of the constant C_μ for gas–particle flows has been discussed by Cao and Ahmadi (1995).

In the k_G equation, the interaction term, Π_{k_G}, represents the energy necessary to accelerate the particles, or the energy transferred from the particles to the gas phase if the particles have high fluctuation velocities in a region where the gas phase turbulent kinetic energy is low. The present formulation assumes the turbulent production in the wakes behind particles to be in local equilibrium with the viscous dissipation, i.e. the particles are assumed to be smaller than the Kolmogorov scale in the gas phase.

When applying the k_G–ϵ_G model presented in this section, one should also be aware of the treatment of the wall region. It has been shown experimentally, e.g. Rashidi *et al.* (1990), that, when particles agglomerate in the wall region, the flow is disturbed. Rizk and Elghobashi (1989) observed numerically that the law of the wall does not hold true even when the suspension is very dilute. Some authors, e.g. Bolio *et al.* (1995), recommend the use of low Reynolds number k_G–ϵ_G models, but this method is also questionable, as damping functions must be expressed for gas–solid suspensions.

More research is needed in order to accurately predict the gas phase turbulence in two-phase flows. A broader discussion on gas-phase turbulence models for gas–particle flows is given by Peirano and Leckner (1997).

5.5. Turbulence models for the particulate phase

Turbulence models for the particulate phase available in the literature are based on the kinetic theory of granular flow. This treatment of the particulate phase uses classical results from the kinetic theory of dense gases, cf. Chapman and Cowling (1970), in combination with Grad's theory, cf. Grad (1949) and a linear theory developed by Jenkins and Richman (1985). The results of Jenkins and Richman are valid for granular flows without an interstitial gas, but Balzer *et al.* (1995) generalized the kinetic theory of granular flow to gas–particle flows. A brief outline of this theory is presented here. Note that, in the present section, the indices i and j are tensor indices.

The particulate phase is modelled as a population of identical, smooth and inelastic spheres. A conservation equation can be formulated in terms of the single particle velocity distribution function $f^{(1)}(\mathbf{x}, \mathbf{c}, t)$ to yield the Maxwell–Boltzmann equation

$$\frac{\partial f^{(1)}}{\partial t} + \frac{\partial}{\partial x_i}(c_i f^{(1)}) + \frac{\partial}{\partial c_i}(F_i f^{(1)}) = \left.\frac{\partial f^{(1)}}{\partial t}\right|_{\text{coll}}, \qquad [125]$$

where c_i is the particle velocity, $F_i = g_i - (c_i - \tilde{u}_{Gi})/\tau^{\lambda}_{Gp} - (\partial \tilde{p}/\partial x_i)/\rho_p$ is the external force per unit of mass acting on a sphere and $\partial f^{(1)}/\partial t|_{\text{coll}}$ is the rate of change of the distribution function owing to particle collisions. The ensemble-averaged value of a function $\psi(\mathbf{c})$ is defined by

$$\langle \psi(\mathbf{c}) \rangle = \frac{1}{n_p} \int \psi(\mathbf{c}) f^{(1)}(\mathbf{x}, \mathbf{c}, t) \mathrm{d}c, \qquad [126]$$

where $\mathrm{d}c$ denotes an element of volume in the velocity-space surrounding the point $\mathbf{c}$ and n_p is the number of particles per unit volume, defined by the integral of the single particle velocity distribution function over the whole velocity domain. Multiplying [125] by $\psi(\mathbf{c})$ and integrating over the velocity domain, one can obtain a transport equation for $\langle \psi(\mathbf{c}) \rangle$, as proposed by Chapman and Cowling (1970)

$$\frac{\partial}{\partial t}(n_p \langle \psi \rangle) + \frac{\partial}{\partial x_i}(n_p \langle \psi c_i \rangle)$$

$$-n_p\left(\left\langle \frac{\partial \psi}{\partial t} \right\rangle + \left\langle c_i \frac{\partial \psi}{\partial x_i} \right\rangle + \left\langle F_i \frac{\partial \psi}{\partial c_i} \right\rangle\right) = C(\psi), \qquad [127]$$

where $C(\psi)$ is the collisional rate of change for ψ and is defined by

$$C(\psi) = \int \psi \left.\frac{\partial f^{(1)}}{\partial t}\right|_{\text{coll}} \mathrm{d}c. \qquad [128]$$

This term represents the integral, over all possible collisions, of the change of ψ due to a binary collision multiplied by the probability of such a collision. According to Jenkins and Richman (1985), $C(\psi)$ can be expressed by

$$C(\psi) = \chi(\psi) - \frac{\partial}{\partial x_i}\theta_i(\psi) - \frac{\partial U_{pj}}{\partial x_i}\theta_i\left(\frac{\partial \psi}{\partial C_j}\right). \qquad [129]$$

The source term, $\chi(\psi)$, represents the loss of the property ψ due to inelastic collisions, and the flux term, $\theta_i(\psi)$, represents the transport of the property ψ during collision. Note that the derivative in the parenthesis of the last term is an argument to the function θ_i.

The rank of the tensor $\theta_i(\psi)$ equals one plus the rank of the argument ψ. Thus, the rank of $\theta_i(\partial\psi/\partial C_j)$ is a tensor of rank three if ψ is a vector. The source and flux terms are defined by integrals involving the pair distribution function, $f^{(2)}(\mathbf{x}_1, \mathbf{x}_2, \mathbf{c}_1, \mathbf{c}_2, t)$, and can be calculated analytically using a linear theory, cf. Jenkins and Richman (1985), in combination with Grad's theory, cf. Grad (1949). In this derivation, the pair distribution function is expressed as the product of the single velocity distribution functions corrected by a factor $g_0 \geqslant 1$, according to the kinetic theory of dense gases, cf. Chapman and Cowling (1970). This factor accounts for the fact that the velocities of two colliding particles are not statistically independent. An expression for this factor in the case of granular flows is given by Lun and Savage (1986) as $g_0 = (1 - \alpha_p/\alpha_{p,\max})^{-2.5\alpha_{p,\max}}$.

A transport equation for the moment of order q, $M_{ij\ldots q} = \langle C_i C_j \ldots C_q \rangle$ with the fluctuation velocity $\mathrm{C_i} = \mathrm{c_i} - \langle \mathrm{c_i} \rangle$, can be obtained from [127] in combination with [129] using $\psi = C_i C_j \ldots C_q$, where m is the mass of a single particle. Noting that $\alpha_p \rho_p = n_p m$, the continuity and momentum equations can be obtained using $\psi = 1$ and $\psi = C_i$, respectively. These equations are identical to

[46] and [114]. The collisional stress tensor $\alpha_p\bar{\bar{\tau}}_p^{X_p} = -\theta_j(mC_i)$ is derived using the procedure described in the previous paragraph to yield

$$\alpha_p\bar{\bar{\tau}}_p^{X_p} = -2\alpha_p^2\rho_p g_0(1+e)T\bar{\bar{I}} - \frac{4}{5}\alpha_p^2\rho_p g_0(1+e)(\bar{\bar{M}} - T\bar{\bar{I}})$$

$$+\frac{4}{5}\alpha_p^2\rho_p d_p g_0(1+e)\sqrt{\frac{T}{\pi}}\,(2\bar{\bar{S}}_p + (\nabla\cdot\mathbf{U}_p)\bar{\bar{I}}), \qquad [130]$$

where $\bar{\bar{M}} = M_{ij} = \langle C_iC_j\rangle$, e is the restitution coefficient and $T = \langle C_iC_i\rangle/3$ is the so-called granular temperature. The restitution coefficient represents the loss of energy during collision and varies between zero and one. If it is equal to one, there is no energy loss during collision (elastic collision); otherwise, energy is dissipated during collision (inelastic collision).

In [130], the second order moment of the particulate phase, $\bar{\bar{M}}$, and the granular temperature, T, must be modelled. The second order moment is modelled using a Boussinesq approximation and the closure model of Jenkins and Richman (1985) to yield

$$\bar{\bar{M}} = T\bar{\bar{I}} - 2\nu_p^t(\bar{\bar{S}}_p - \tfrac{1}{3}(\nabla\cdot\mathbf{U}_p)\bar{\bar{I}}), \qquad [131]$$

where the turbulent viscosity of the particulate phase can be expressed as

$$\nu_p^t = \left(\frac{1}{3}\tau_{Gp}^t k_{Gp} + \frac{1}{2}\tau_{Gp}^x T(1+\alpha_p g_0\phi_c)\right)\Big/\left(1 + \frac{\tau_{Gp}^x}{2}\frac{\sigma_c}{\tau_p^c}\right), \qquad [132]$$

cf. Simonin (1995) and Peirano and Leckner (1997). The time scale τ_{Gp}^t is the interaction time between particle motion and gas phase fluctuations. This time scale can be calculated according to Csanady (1963) as $\tau_G^t(1 + C_\beta(3U_{rel}^2/2k_G))^{-1/2}$. The time scale of the large eddies, τ_G^t, is defined by $C_\mu(3k_G/2\epsilon_G)$. The relative velocity $\mathbf{U}_{rel}$ is defined by [116] and the constant C_β depends on the direction in the flow, cf. Simonin (1995). The constants ϕ_c and σ_c are defined by $2(1+e)(3e-1)/5$ and $(1+e)(3-e)/5$, respectively. The collisional stress tensor, defined by [130], can now be rewritten as

$$\alpha_p\bar{\bar{\tau}}_p^{X_p} = -\tfrac{1}{3}\alpha_p\mathrm{tr}(\bar{\bar{\tau}}_p^{X_p})\bar{\bar{I}} + 2\alpha_p\rho_p\nu_p^c(\bar{\bar{S}}_p - \tfrac{1}{3}(\nabla\cdot\mathbf{U}_k)\bar{\bar{I}}), \qquad [133]$$

where the collisional viscosity, ν_p^c, is defined by

$$\nu_p^c = \frac{4}{5}\alpha_p g_0(1+e)\left(\nu_p^t + d_p\sqrt{\frac{T}{\pi}}\right). \qquad [134]$$

The effective stress tensor can now be written as

$$\alpha_p(\bar{\bar{\tau}}_p^{X_p} + \bar{\bar{T}}_p^{Re}) = -(P_p - \xi_p\nabla\cdot\mathbf{U}_k)\bar{\bar{I}} + 2\mu_p(\bar{\bar{S}}_p - \tfrac{1}{3}(\nabla\cdot\mathbf{U}_k)\bar{\bar{I}}), \qquad [135]$$

where the fluctuation stress tensor of the particulate phase is $\bar{\bar{T}}_p^{Re} = -\rho_p\bar{\bar{M}}$, the effective pressure is

$$P_p = \alpha_p\rho_p T(1 + 2\alpha_p g_0(1+e)) \qquad [136]$$

and the bulk viscosity is

$$\xi_p = \frac{4}{3}\alpha_p^2\rho_p d_p g_0(1+e)\sqrt{\frac{T}{\pi}}. \qquad [137]$$

The shear viscosity is given as the sum of a turbulent viscosity and collisional viscosity, $\mu_p = \alpha_p\rho_p(\nu_p^t + \nu_p^c)$. Finally, a transport equation for the granular temperature, or for the turbulent kinetic energy of the particulate phase, $k_p = 3T/2$, is required. This is given by

$$\alpha_p\rho_p\frac{D_p}{Dt}k_p = \frac{\partial}{\partial x_i}\left(\alpha_p\rho_p(K_p^t + K_p^c)\frac{\partial k_p}{\partial x_i}\right) - \sum_{ij}\frac{\partial U_{pi}}{\partial x_j}$$

$$-\frac{2\alpha_p\rho_p}{\tau_{Gp}^x}(2k_p - k_{Gp}) + \alpha_p\rho_p\frac{e^2-1}{3\tau_p^c}k_p, \qquad [138]$$

where K_p^t and K_p^c are the turbulent and collisional diffusivity coefficients, respectively, and Σ_{ij} denotes the effective stress tensor, $-\alpha_p(\bar{\bar{\tau}}_p^{X_p} + \bar{\bar{T}}_p^{Re})$. The time scale $\tau_p^c = (d_p/24g_0\alpha_p)\sqrt{\pi/T}$ is the particle–particle collision time, i.e. the time between two consecutive binary collisions for a given particle. The gas–particle covariance, k_{Gp}, is defined as $\langle C_i u_{Gi}'' \rangle$, where $u_{Gi}'' = u_{Gi} - \langle u_{Gi} \rangle^{X_p \rho_p}$.

The turbulent diffusivity is modelled as

$$K_p^t = \left(\frac{3\tau_{Gp}^t}{5\tau_{Gp}^x} k_{Gp} + T(1 + \alpha_p g_0 \varphi_c) \right) \Bigg/ \left(\frac{9}{5\tau_{Gp}^x} + \frac{\xi_c}{\tau_p^c} \right), \tag{139}$$

where $\varphi_c = 3(1 + e)^2(2e - 1)/5$ and $\xi_c = (1 + e)(49 - 33e)/100$. The collisional diffusivity, K_p^c, is defined by

$$K_p^c = \alpha_p g_0 (1 + e) \left(\frac{6}{5} K_p^t + \frac{4}{3} d_p \sqrt{\frac{T}{\pi}} \right). \tag{140}$$

To solve [138], a semi-empirical equation for the gas–particle covariance was suggested by Simonin (1995)

$$\alpha_p \rho_p \frac{D_p}{Dt} k_{Gp} = \frac{\partial}{\partial x_j} \left(\alpha_p \rho_p \frac{\nu_{Gp}^t}{\sigma_{k_G}} \frac{\partial k_{Gp}}{\partial x_j} \right) - \alpha_p \rho_p \langle u_{Gi}'' u_{pj}' \rangle \frac{\partial U_{pi}}{\partial x_j}$$

$$- \alpha_p \rho_p \langle u_{Gj}'' u_{pi}' \rangle \frac{\partial U_{Gi}}{\partial x_j} - \alpha_p \rho_p \epsilon_{Gp} + \Pi_{Gp}, \tag{141}$$

where the dissipation rate, ϵ_{Gp}, is given by $\epsilon_{Gp} = k_{Gp}/\tau_{Gp}^t$, and the gas–particle turbulent viscosity is $\nu_{Gp}^t = k_{Gp}\tau_{Gp}^t/3$. The interaction term, Π_{Gp}, is given by

$$\Pi_{Gp} = -\frac{\alpha_p \rho_p}{\tau_{Gp}^x} ((1 + X_{Gp}) k_{Gp} - 2k_G - 2X_{Gp} k_p), \tag{142}$$

where $X_{Gp} = \alpha_p \rho_p / \alpha_G \rho_G$.

The model of Jenkins and Richman (1985) as well as the generalized model of Simonin (1995) are derived for certain restricted conditions. The primary restrictions are granular flows with small spatial gradients for the mean fields (velocity and granular temperature), a low level of anisotropy and nearly elastic particles ($1 - e$ must be small) in translational motion. In reality, the particle flow contains rough, rotating particles, and an accurate collision model should account for these effects, cf. Foerster *et al.* (1994). A formulation of the kinetic theory of granular flow for slightly elastic, slightly rough spheres has been given by Lun (1991), but it has not been generalized to granular flow taking into account the interstitial gas. Furthermore, there is no general formulation of the transverse forces acting on a single particle in a suspension. The kinetic theory of granular flow presented in this section is fairly free from empirical constants. The only constants that appear directly in the model are the restitution coefficient, e, and the radial distribution function, g_0, although gas phase turbulence constants affect the model indirectly, through the correlation, k_{Gp}, between the fluctuating motion of the gas and particle phases. As far as the restitution coefficient is concerned, its value affects the results significantly in numerical simulations of dense suspensions, Balzer *et al.* (1995), while the influence is small for dilute suspensions, Bolio *et al.* (1995). For dense suspensions, a decrease of the restitution coefficient causes the granular temperature to decrease. This in turn causes a decrease of the viscosity and diffusion, resulting in larger gradients and more bubbles in the calculated results. However, the restitution coefficient has a physical meaning and has a constant value for a given material. Measured restitution coefficients for different types of materials are given by Foerster *et al.* (1994).

The kinetic theory presented in this section takes the interstitial gas into account and is thus a generalization of the results of Jenkins and Richman. For a dilute suspension, i.e. where $\tau_p^c \gg \tau_{Gp}^x$, the particle mean free path is limited by the aerodynamic forces, cf. Boelle *et al.* (1995). Some kinetic theory models omit the aerodynamic forces, cf. section 6.2. A direct consequence of this is an overprediction of the particle viscosity in dilute regions. This matter is also discussed by Peirano *et al.* (1997).

A detailed derivation of the kinetic theory of granular flow, outlined briefly above, is given by Peirano and Leckner (1997).

5.6. Concluding remarks on turbulence

As pointed out by Simonin (1995), for dilute suspensions, the models presented above lead to an overestimation of the normal particle fluctuation stress components perpendicular to the mean flow. For such cases, separate transport equations for the particle second order moment might be needed. However, in dense suspensions, e.g. bubbling fluidized beds, where the collisional mechanism is dominant, the model presented in this section seems to give satisfactory results. In addition, as pointed out by Boelle *et al.* (1994), their k_G–ϵ_G model was originally developed for dilute suspensions. In the case of dense suspensions, several studies have shown that the correlations related to the fluctuations of the gas phase velocity are nearly negligible. According to Balzer *et al.* (1995), turbulent transport in the gas phase has a relatively great effect on the mean flow field in dilute gas–particle flows, for example in the freeboard or inside the gas bubbles of a fluidized bed. In the dense regions surrounding the bubbles, however, the inertia of the particles damps out the high frequency turbulent scales in the gas phase. This has been discussed by several authors, e.g. Rowe (1971) and Kuipiers *et al.* (1992). The turbulence of the particulate phase in the dense regions is generated mainly by particle collisions, whereas the main generation mechanism in the dilute regions is interaction with the turbulent eddies of the gas phase. This implies that the application of a two-fluid model to a bubbling fluidized bed may require a model simultaneously taking into account the turbulent transport, drag and particle–particle collisions.

6. APPLICATIONS TO FLUIDIZATION

A number of publications on simulation of the hydrodynamics of bubbling and circulating fluidized beds can be found in the literature. Tables 6 and 7, respectively, summarize work on bubbling and circulating fluidization simulations. Investigations of pneumatic conveying are not considered in this study.

The tables show details about the model itself, describe some computational aspects, the name of the code and validation method, and give some general comments. The model column describes the treatment of the phasic stress tensors, the particle pressure and drag function, and states whether the simulation was two or three-dimensional. The computations column summarizes the mean particle diameter, particle density, computational mesh size, time step and simulation time. In some cases, simulation time was not given in the publications, and the values presented in the tables were then inferred from the latest point in time from which results were presented. In the comments column, it is stated whether a symmetry assumption is made on the flow field and, for the Illinois Institute of Technology/Argonne National Laboratory (IIT/ANL) group, whether model A or B is used, cf. section 6.1. The remaining groups use model A.

The codes used and the specific cases simulated by the different groups vary considerably, which makes it difficult to compare the different methods. However, an attempt has been made to outline the main features of each groups' work, bearing in mind that there may be other important aspects that affect the solution, such as boundary conditions, initial conditions and numerical dissipation.

6.1. Bubbling fluidized beds

The material found on bubbling fluidization has essentially been produced by seven different research groups over the past 15 years.

The members of the IIT/ANL group are pioneers in the field and have published the greatest amount of articles, using a code which is based on the K-FIX code, originally developed by Rivard and Torrey (1977). The earlier publications by the IIT/ANL group are based on inviscid laminar models of both phases using a 2D model. Later work takes into account the turbulence in the particulate phase using a kinetic theory model that does not include the aerodynamic forces, and 3D calculations are also made. The IIT/ANL group introduces two different treatments of the gas pressure gradient in the momentum equations. In model A, the pressure gradient is included in each of the phasic momentum equations. This is the model presented in section 4.3.1, and is the conventional way of treating the gas pressure gradient. In model B, the whole gas pressure gradient

Table 6. Summary of bubbling fluidized bed simulations

References	Model	Computations	Code	Validation	Comments
IIT/ANL					
Gidaspow and Ettehadieh (1983)	Non-viscous, modulus of elasticity Wen and Yu/Ergun 2D	$d_p = 0.503$ mm $\rho_p = 2660$ kg/m^3 $12 \times 31 = 372$ nodes	K-FIX	Time-averaged voidage distribution	Symmetry model A
Ettehadieh *et al.* (1984)	Non-viscous, modulus of elasticity Wen and Yu/Ergun 2D	$d_p = 0.280$ mm $\rho_p = 901$ kg/m^3	K-FIX	Time-averaged velocity and voidage profiles	Symmetry model A
Lyczkowski *et al.* (1987)	Non-viscous, modulus of elasticity Wen and Yu/Ergun 2D	$d_p = 0.503$ mm $\rho_p = 2440$ kg/m^3 $12 \times 31 = 372$ nodes $\Delta t = 10^{-4}$ s	FLUFIX	Video recording	Symmetry model A
Bouillard *et al.* (1989)	Non-viscous, modulus of elasticity Wen and Yu/Ergun 2D	$d_p = 0.503$ mm $\rho_p = 2440$ kg/m^3 $31 \times 48 = 1488$ nodes $\Delta t = 10^{-5}$–10^{-4} s	FLUFIX	Video recording and time-averaged voidage distribution	Symmetry model A/B
Lyczkowski *et al.* (1989)	Constant gas and particulate phase viscosities, modulus of elasticity Wen and Yu/Ergun 2D	$d_p = 0.500$ mm $\rho_p = 2440$ kg/m^3 $15 \times 48 = 720$ nodes $\Delta t = 8 \times 10^{-5}$–$10^{-4}$ s $T_{sim} = 4$ s	FLUFIX	Time-averaged voidage tube erosion	Symmetry model A/B
Ding and Gidaspow (1990)	Laminar gas phase and kinetic theory for particulate phase, Wen and Yu/Ergun 2D	$d_p = 0.500$ mm $\rho_p = 2500$ kg/m^3 $16 \times 42 = 672$ nodes $\Delta t = 5 \times 10^{-5}$ s $T_{sim} = 5$ s	IFAP	Time-averaged voidage	No symmetry model A
Lyczkowski *et al.* (1991)	Constant gas and particulate phase viscosities, modulus of elasticity Wen and Yu/Ergun 2D	$d_p = 0.500$ mm $\rho_p = 2490$ kg/m^3 $32 \times 80 = 2560$ nodes $\Delta t = 5 \times 10^{-4}$ s $T_{sim} = 4$ s	FLUFIX	Pressure fluctuation spectra, time-averaged solids, velocity	No symmetry model B
Ding and Lyczkowski (1992)	Laminar gas phase and kinetic theory for particulate phase, Wen and Yu/Ergun 3D	$d_p = 1.0$ mm $\rho_p = 2580$ kg/m^3 $4 \times 10 \times 33 = 1320$ nodes $\Delta t = 5 \times 10^{-4}$ s $T_{sim} = 2$ s	IFAP	Tube erosion	Symmetry model A
Gamwo *et al.* (1995)	Constant gas and particulate phase viscosities, modulus of elasticity Wen and Yu/Ergun 3D	$d_p = 0.503$ mm $\rho_p = 2610$ kg/m^3 $8 \times 14 \times 38 = 4256$ nodes $\Delta t = 10^{-5}$–4×10^{-4} s	IFAP3DB	—	Symmetry model B

Table 6—*continued.*

References	Model	Computations	Code	Validation	Comments
EG&G/DOE					
Syamlal and O'Brien (1989)	Non-viscous, solving for particle pressure instead of voidage locally, Syamlal and O'Brien 2D	$d_p = 0.020$–0.200 mm $\rho_p = 2500$ kg/m^3 $\Delta t = 10^{-4}$ s $T_{sim} = 1.3$ s	—	Bubble frequency, velocity, wake angle, wake fraction, pressure profile	Symmetry
TU					
Kuipers *et al.* (1992a)	Non-viscous, modulus of elasticity, Wen and Yu/Ergun 2D	$d_p = 0.500$ mm $\rho_p = 2660$ kg/m^3 $38 \times 100 = 3800$ nodes $\Delta_t = 2.5 \times 10^{-4}$ s $T_{sim} = 1.05$ s	—	—	Symmetry thermal calculations
Kuipers *et al.* (1992b)	Constant gas and particulate phase viscosities, modulus of elasticity Wen and Yu/Ergun 2D	$d_p = 0.500$ mm $\rho_p = 2660$ kg/m^3 $76 \times 80 = 6080$ nodes $\Delta t = 3 \times 10^{-4}$ s $T_{sim} = 0.72$ s	—	—	Symmetry
Kuipers *et al.* (1993)	Constant gas and particulate phase viscosities, modulus of elasticity Wen and Yu/Ergun 2D	$d_p = 0.500$ mm $\rho_p = 2660$ kg/m^3 $38 \times 100 = 3800$ nodes variable Δt $T_{sim} = 0.798$ s	—	Video recording	Symmetry
Nieuwland *et al.* (1996)	Constant gas and particulate phase viscosities, modulus of elasticity, Wen and Yu/Ergun 2D	Varying d_p Varying ρ_p 3040–12160 nodes $\Delta t = 10^{-4}$–1.25×10^{-4} s $T_{sim} = 0.25$ s	—	Video recording, bubble size, leakage fraction, bubble shape factor	Symmetry
NYU					
Li and Zakkay (1995)	Non-viscous, modulus of elasticity, Wen and Yu/Ergun 2D	$d_p = 1.5$ mm $\rho_p = 2490$ kg/m^3 2496–4992 nodes $\Delta t = 10^{-5}$ s $T_{sim} = 2.0$ s	—	—	Symmetry
RWTH					
Boemer *et al.* (1995)	Laminar for gas phase and kinetic theory for particulate phase, Syamlal *et al.* 2D	$d_p = 0.5$ mm $\rho_p = 2660$ kg/m^3 $30 \times 79 = 2370$ nodes $T_{sim} = 2.0$ s	FLUENT 4.23	Time-averaged voidage	Symmetry

Table 6—*continued.*

References	Model	Computations	Code	Validation	Comments
EDF					
Balzer *et al.* (1995)	k–ϵ for gas phase and kinetic theory for particulate phase, Wen and Yu/Ergun 2D	$d_p = 0.5$ mm $\rho_p = 2500$ kg/m^3 $50 \times 100 = 5000$ nodes $T_{sim} = 5$ s	MELODIF	X-ray image, pressure distribution, bubble diameter, bed height	No symmetry
CTH					
Enwald *et al.* (1997)	Laminar gas phase and kinetic theory for particulate phase modulus of elasticity, Gibilaro, 2D	$d_p = 0.7$ mm $\rho_p = 2600$ kg/m^3 $30 \times 112 = 3360$ nodes $\Delta t = 10^{-5}$ s $T_{sim} = 32$ s	GEMINI2D	Capacitance probe measurements of statistical bubble parameters	No symmetry, both atmospheric and pressurized conditions

Table 7. Summary of circulating fluidized bed simulations

References	Model	Computations	Code	Validation	Comments
IIT/ANL					
Tsuo and Gidaspow (1990)	Constant gas and particulate phase viscosities, modulus of elasticity, Wen and Yu/Ergun, 2D	$d_p = 0.076$ mm $\rho_p = 1714$ kg/m^3 $30 \times 38 = 1140$ nodes $\Delta t = 5 \times 10^{-4}$ s $T_{sim} = 18$ s	Extension of K_FIX	Radial solids volume fraction distribution, axial gas and solids velocity distribution	Model B
Gidaspow and Therdthianwong (1993)	Kinetic theory and LES for gas phase Wen and Yu/Ergun 2D	$d_p = 0.210$ mm $\rho_p = 1530$ kg/m^3	Extension of K-FIX	—	Model B
Wang and Bouillard (1993)	Constant gas and particulate phase viscosities modulus of elasticity Wen and Yu/Ergun 2D	$d_p = 0.090$ mm $\rho_p = 6700$ kg/m^3	FLUCOMP	—	Model B
Tel-Tek/HiT-TF					
Mathiesen *et al.* (1996)	Kinetic theory with several particle size and LES for gas phase Wen and Yu/Ergun 2D	$d_p = 0.040$–0.170 mm $\rho_p = 2500$ kg/m^3 $38 \times 102 = 3876$ nodes $T_{sim} = 60$ s	FLOTRACS-MP-3D	Particle and mean particle diameter, axial velocity fluctuations, mean velocity profiles	
RWTH					
Boemer *et al.* (1994)	Kinetic theory cluster correction for drag 2D	$d_p = 0.074$ mm $\rho_p = 1770$ kg/m^3 $36 \times 60 = 2160$ nodes $T_{sim} = 8.0$ s	FLUENT 4.23	Radial solids volume fraction	
EDF					
Balzer *et al.* (1996)	Kinetic theory and k–ϵ for gas phase Wen and Yu/Ergun 3D	$d_p = 0.140$ mm $\rho_p = 2500$ kg/m^3 $T_{sim} = 30$ s	ASTRID	Vertical pressure profile	

is placed in the gas phase and the expression for the drag function is modified accordingly, cf. Bouillard *et al.* (1989). The IIT/ANL group's motivation for using model B is that it makes the set of equations well-posed. However, this has been shown only in the form of a one-dimensional, initial-value problem Lyckowski *et al.* (1978). To our knowledge, nobody has yet proven the well-posedness for a multi-dimensional initial-boundary value problem, and consequently most researchers today prefer model A.

In the code by the EG&G W. A. S. C. Inc./Department of Energy Morgantown (EG&G/DOE) group, the particle pressure is set to zero in all parts of the bed except for the very dense regions. In these regions, the voidage is fixed to a value that corresponds to the maximum particle packing, and the particle pressure is calculated to match this value in the particle momentum equation. This approach assumes an interpretation of the particle pressure as a repulsive force between the particles in the dense regions, similar to that of the modulus of elasticity concept, cf. [63]. The authors use their own drag correlation, cf. [92].

The Twente University (TU) group adopted a modelling approach similar to that of the IIT/ANL group and has contributed to an increased knowledge of heat transfer modelling in bubbling fluidized beds.

The New York University (NYU) group coupled an inviscid hydrodynamic model with different tube erosion models. Erosion rates were calculated on tube banks using a Cartesian mesh and blocked cells to approximate circular tube geometries.

The Rheinisch-Westfälische Technische Hochschule (RWTH) group developed the FLUENT code in cooperation with FLUENT Europe to simulate gas–particle flows and applied the code to both bubbling and circulating fluidization. The model is based on the kinetic theory of granular flow. The contribution of the group is mainly a comparison of different stress tensor models and comparisons between algebraic and differential models for the granular temperature. The group has also tested different drag models and has chosen to use the correlation of Syamlal and O'Brien, cf. [92] for bubbling fluidized bed simulations.

The most complete analysis of the two-fluid model and constitutive equations applied to gas–particle fluidization has been made by the Electricité de France (EDF) group. Their kinetic theory model takes into account the influence of the gas phase, which makes the model applicable for all particle concentrations. A complete turbulence model for both phases is used, i.e. four coupled transport equations are solved, cf. section 5. Some work has been done on three-dimensional simulations.

A number of the above workers assume a symmetrical flow field in the bed and solve only for half the bed width in order to save computational time, cf. table 6. An experimental validation of such results requires a well-defined experiment in which a single bubble rises through the bed without any significant disturbances. In reality, fluidization is a chaotic process with strong bubble interaction and a highly asymmetrical flow pattern. Thus, in order to compare results of the numerical simulations with the experimental results, statistical averages of the different flow parameters must be calculated over quite a significant period of time, without any symmetry assumptions being made. This approach has been used by the Chalmers Tekniska Högskola (CTH) group, cf. Enwald *et al.* (1997), using a time-averaging period of 32 s. Two models have been used in this work. The first model is defined by the phasic continuity and momentum equations [46–47], with Newtonian phasic stress models [49–51], where the viscosity for each phase is constant. The particle–particle interaction force model is expressed with [62–63] and [65], and the drag function model suggested by Gibilaro [106], is introduced in the momentum equation as described in section 4.4. The second model is also defined by [46–47] with the drag function model of Gibilaro [106]. However, the Newtonian phasic stress model [49–51], is used only for the gas phase while, for the particulate phase, the kinetic theory of granular flow is introduced. For the particulate phase, the stress tensor is given by [135] and the granular temperature is computed with [138] where gas phase turbulence is neglected. A time sequence of bubbles rising up through the bed, calculated from the two-dimensional form of the constant viscosity model is presented in figure 12. Instantaneous gas and particle velocities are shown in figure 13. As shown in the figures, the flow is stochastic, with strong bubble interactions including both coalescence and split-up. Experimental measurements of visible bubble flow parameters and the through-flow velocity of gas through the bubbles were carried out in a freely bubbling pressurized model bed having the same geometry as

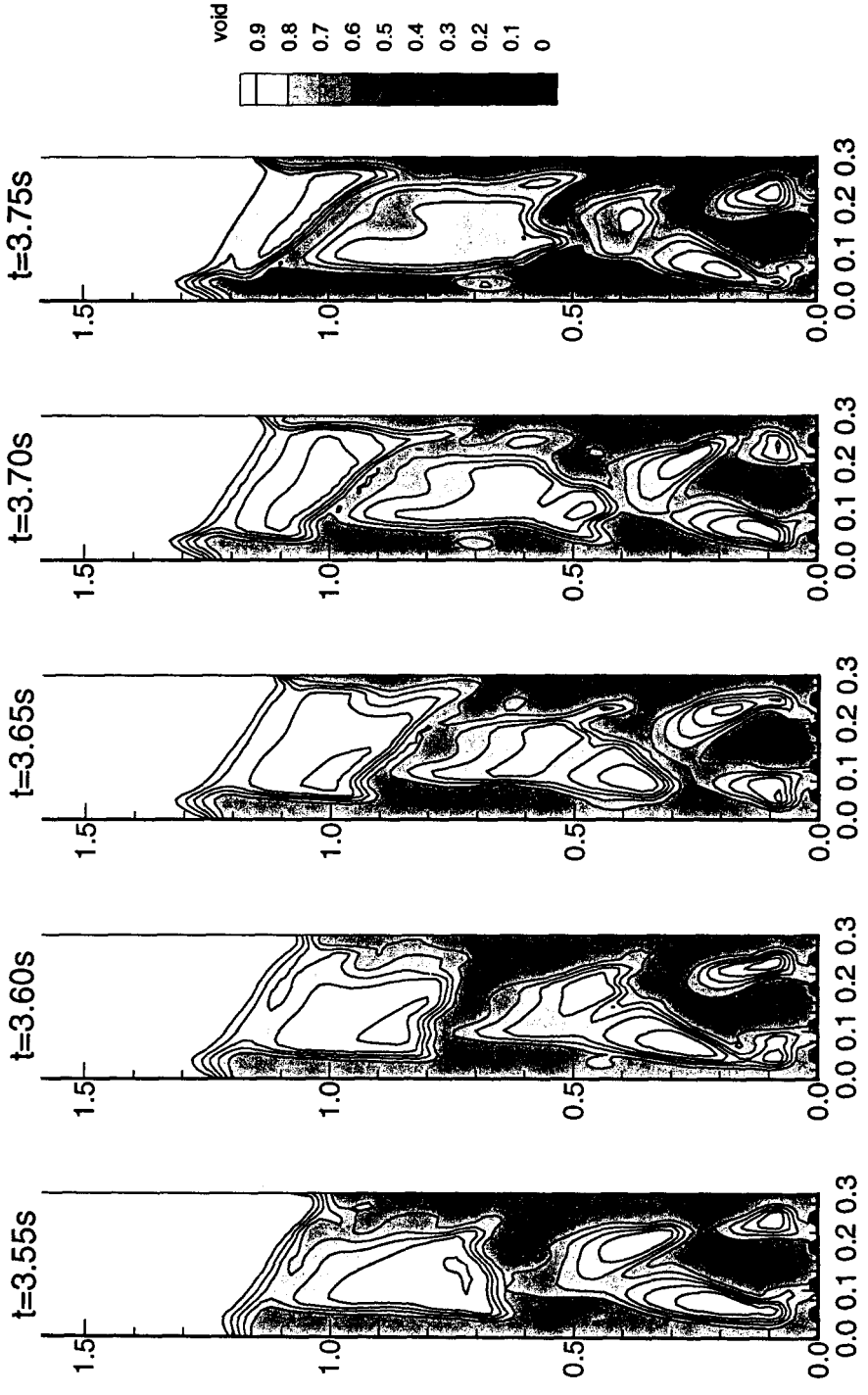

Figure 12. Time sequence of voidage distribution.

that used in the numerical simulations. Further details on the comparisons between the experimental and numerical results are reported by Enwald and Almstedt (1997).

Many of the published works have used a constant viscosity for the particulate phase. This means that the influence of voidage on the viscosity is not taken into account. One simple way of doing this would be to couple a voidage-dependent mixture viscosity model, e.g. one of the models given by [58]–[61], to the particle viscosity, using a relation of the type suggested in [52]. However, the physical justification for [52] is questionable and, to our knowledge, this approach has not been tried by any of the groups. In the granular flow theory, the influence of voidage on the particulate phase viscosity is taken into account by the use of the effective stress tensor. This is a physically more sound approach, although the models contain a number of empirical constants that need to be determined experimentally. Thus, the proof of the pudding is in the eating, and any model used should be carefully verified versus experiments. It should also be noted in this connection that the majority of the simulations thus far has been made two-dimensionally, something that may affect the numerical results to be compared with the three-dimensional reality.

6.2. *Circulating fluidized beds (CFB)*

There are two major applications of CFB technology: circulating fluidized beds for catalytic cracking and circulating fluidized bed combustors. In this section, we have selected papers on circulating fluidized bed combustor simulations of real boilers and pilot scale plants.

The IIT/ANL group initiated two-dimensional computations of circulating fluidized beds using constant gas and particle phase viscosities. This was later improved by using kinetic theory of granular flow and large eddy techniques (LES) for the gas phase. The kinetic theory as used by the IIT/ANL group does not take aerodynamic forces into account, however, and may therefore lead to an overprediction of the particle phase viscosity for dilute suspensions, as discussed in section 5.5. Furthermore, the use of the LES technique in a 2D model is questionable, as large scale eddies are always three-dimensional.

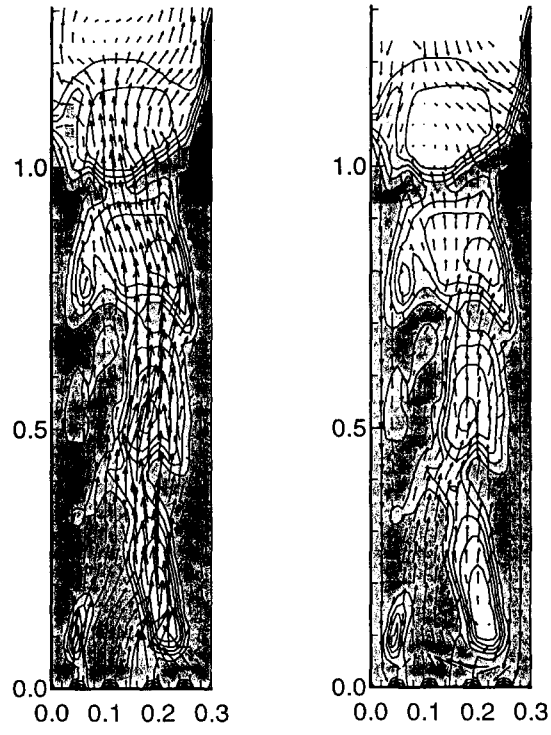

Figure 13. Instantaneous voidage distribution, gas velocity field (left) and particle velocity field (right) after 4 s.

The Telemark Technological R&D Centre/Telemark Institute of Technology (Tel-Tek/HiT-TF) group made the first simulation on two-dimensional multi-phase (three particle sizes—four phases) fluidization in a CFB. Their model is based on the model by Jenkins and Mancini (1987), which is a generalization of the kinetic theory of granular flow presented in section 5.5. The simulations seem to predict segregation effects fairly well. The use of LES for the gas phase is questionable for the same reason as is given for the IIT/ANL group.

The research group at RWTH has performed two-dimensional simulations using the kinetic theory of granular flow without taking into account the turbulence in the gas phase. A drag function model with a cluster correction by O'Brien and Syamlal is used, cf. [92]–[94] and [101]. It is not obvious why the clustering effect should be included in the drag correlation, as this effect is already accounted for by the transport equations.

The EDF group has made three-dimensional simulations of industrial units using the set of equations presented in section 5. Their validation of the time-averaged vertical pressure profile over a period of 30 s shows that the dense region at the bottom of the combustion chamber is not well-predicted. Generally, the model appears to predict the mean flow field fairly well.

Most of the published work on CFB simulations included here applies the kinetic theory of granular flow without taking into account the influence of the gas phase. As discussed above, this approximation is rather crude in the dilute parts of the suspension and leads to an erroneous value of the particulate phase viscosity. In addition, most groups do not account for the turbulent coupling between the phases, i.e. that the particles are dispersed by gas phase turbulence and also modulate the gas phase turbulence. This effect is included in the model used by the EDF group, cf. the set of equations presented in section 5. The effect of this on the solutions is not clear and, again, the different models must be validated versus experiments.

7. CONCLUSIONS

This report describes the steps needed to derive a closed two-fluid model applicable to non-reacting gas-particle flows. Two types of models are described. The first type, derived by a traditional approach, does not include any turbulence models. In the second type, turbulence is modelled for both the gas and particulate phases. A full derivation is presented for the model obtained with the traditional approach, whereas only a brief overview is given for the turbulent two-fluid model.

The first set of balance equations described in the present report, i.e. the local instantaneous equations and corresponding jump conditions, completely describes the dynamics of both phases. As mentioned in section 1.5, these equations could in theory be solved either by direct simulation or by using a Lagrangian description for the particulate phase. However, with today's computer capacity, both approaches would result in completely unrealistic simulation times if the number of particles in the system is large. Thus, an averaged, Eulerian, approach is often required, which, however, necessitates the inclusion of additional expressions to close the set of equations.

To close the averaged transport equations, constitutive laws and transfer laws are needed. An important area of future work is to improve the constitutive laws, e.g. the shear stress models for the respective phases. Transfer laws are needed to model the interfacial relations, of which only interfacial momentum is treated in this report. The interfacial momentum transfer was rewritten into a generalized drag, $\mathbf{M}_{kl}^{d}$, which is contributed to by the stationary drag, added mass, transverse, history and other forces. For suspensions with a small gas-to-particle density ratio, such as gas-fluidized beds, the only one of these forces included in the two-fluid models is normally the stationary drag, while the remaining forces are neglected. The correlations given in this report for the drag function, K, used when calculating the stationary drag force should be employed with caution, as most of them are derived from homogeneous fluidization experiments, i.e. from liquid–particle fluidized beds, and not from heterogeneous fluidization. Furthermore, if a stringent derivation of an Eulerian turbulent two-phase flow model is made, a drift velocity is introduced in the expression for the interfacial drag term, cf. [116] and [117]. This velocity represents the dispersion of particles by large-scale turbulent eddies and is likely to be important for cases with small particles, although many groups use turbulence models without including the drift velocity.

The two-fluid model equations must be solved together with appropriate boundary conditions. Problems related to the boundary conditions are, for instance, how to model the particle motion at the walls and how to model the air distributor plate, for both phases. The latter problem depends on the physical geometry of the distributor plate. Boundary conditions have not been discussed in this paper.

An area that needs improvement is the mathematical theory of well-posedness for systems of partial differential equations describing gas–particle flows. The well-posedness of such problems has been studied by e.g. Lyczkowski *et al.* (1982) for a one-dimensional inviscid model formulated as an initial-value problem, using Lax's theorem (1958). It was found that this inviscid, one-dimensional initial-value problem can be well-posed under some conditions, which does not, however, prove the well-posedness in several dimensions or when the effects of the boundary conditions are included (initial-boundary value problem). With the present level of knowledge, there is no way to determine whether the multidimensional two-fluid model is well-posed as an initial-boundary value problem.

The influence of turbulence appears in the equations in the fluctuation correlations introduced by the Reynolds decomposition. For fluidization applications in which both the density difference between the phases and the particle concentration are high, i.e. for bubbling gas-fluidized beds, it seems that the inertia of the particles damps out the turbulence in the gas phase. This has been discussed by several authors, e.g. Rowe (1971) and Kuipiers *et al.* (1992a). Thus, in the dense part of the bed, ignoring the gas phase turbulence may be a valid approximation, whereas in the dilute regions, i.e. in the bubbles and the freeboard, the turbulence may well be of greater importance.

If turbulence is included, the gas-phase turbulence is normally modelled using a modified k–ϵ model. This model includes a number of case-dependent empirical constants. Because of a lack of experimental data, these constants are usually taken from the standard one-phase k–ϵ model. As this model can give significant errors even for a number of single phase flows, its validity in two-phase flow turbulence is, at least, questionable.

The simplest way to implement turbulence in the particulate phase is to include a constant, or voidage-dependent, particle phase viscosity, using a Newtonian stress–strain relation. In the literature, the only voidage dependent viscosity models available are for the mixture viscosity. Thus, if a voidage-dependent viscosity model is to be used, the mixture viscosity must be related to the particle phase viscosity through some physically reasonable assumption. Alternatively, the particle phase turbulence can be modelled with the kinetic theory of granular flow, cf. section 5.5. This theory is sometimes used without taking into account the effects of the interstitial gas on the particulate phase. However, this effect may be important for dilute regions of the flow field.

A critical discussion of different approaches to the modelling of bubbling and circulating fluidized beds is given in section 6. It can be noted that few of the models have as yet been satisfactorily verified versus experimental results. Both the simpler and the more advanced models contain a number of assumptions, and it remains to be investigated which method is the most reliable for fluidized bed applications.

Acknowledgements—The authors would like to express their thanks to the Swedish National Board for Industrial and Technical Development (NUTEK), Elforsk AB, ABB Carbon, Kvaerner Enviropower AB, Stockholm Energi AB, Sydkraft AB and Vattenfall Energisystem AB for their financial support of this work.

REFERENCES

Albråten, P. (1982) The dynamics of two-phase flow. Ph.D. thesis, Department of Energy Conversion, Chalmers University of Technology, Sweden.

Andersson, S. (1991) Dimensionless groups in the momentum equations of a bubbling bed. Report A91-188, Department of Energy Conversion, Chalmers University of Technology, Sweden.

Arnold, G. S., Drew, D. A. and Lahey, R. T. (1989) Derivation of constitutive equations for interfacial force and Reynolds stress for a suspension of spheres using ensemble cell averaging. *Chem. Eng. Comm.* **86,** 43–54.

Arnold, G. S., Drew, D. A. and Lahey, R. T. (1990) An assessment of multiphase flow models using the second law of thermodynamics. *Int. J. Multiphase Flow* **16,** 481–494.

Balzer, G., Boelle, A. and Simonin, O. 1995. Eulerian gas-solid flow modelling of dense fluidized bed. *Fluidization VIII*, Int. Symp. of the Engineering Foundation, Tours, 14–19 May, pp. 1125–1134.

Bel Fdhila, R. and Simonin, O. (1992) Eulerian prediction of a turbulent bubbly flow downstream of a sudden pipe expansion. *Proc. 6th Workshop on Two-phase Flow Predictions*, Erlangen, FRG, pp. 264–273.

Boelle, A., Balzer, G. and Simonin, O. (1995) Second order prediction of the particle phase stress tensor of inelastic spheres in simple shear dense suspensions. *Gas–Solid Flows*, *ASME FED* **228,** 9–18.

Boelle, A., Balzer, G. and Simonin, O. (1994) Application d'une modélisation à deux fluides à la prédiction des lits fluidisés denses. Report HE-44/94/017A, Laboratoire National d'Hydraulique, EDF, Chatou, France.

Boemer, A., Qi, H. and Renz, U. (1994) Modelling of bubble eruption in a fluidized bed with the Eurelian approach. Presented at the 28th IEA-FBC Meeting in Kitakyushu, Japan, 24–25 July.

Boemer, A., Qi, H., Renz, U., Vasquez, S. and Boysan, F. (1995) Eulerian computation of fluidized bed hydrodynamics—a comparison of physical models. *ASME FBC Conf.* **2,** 775–787.

Bolio, E. J., Yasuna, J. A. and Sinclair, J. L. (1995) Dilute turbulent gas–solid flow in riser with particle–particle interactions. *AIChE Journal* **41,** 1375–1388.

Bouillard, J. X., Lyczkowski, R. W. and Gidaspow, D. (1989) Porosity distributions in a fluidized bed with an immersed obstacle. *AIChE Journal* **35,** 908–922.

Bouré, J. A. and Delhaye, J. M. (1982) In *Handbook of Multiphase Systems*, ed. G. Hetsroni, Section 1.2, pp. 1-36–1-95. McGraw-Hill, New York.

Brinkman, H. C. (1952) The viscosity of concentrated suspensions and solutions. *J. Chem. Phys.* **20,** 571–573.

Campbell, C. S. and Wang, D. G. (1991) Particle pressure in gas-fluidized beds. *J. Fluid Mech.* **227,** 495–598.

Cao, J. and Ahmadi, G. (1995) Gas-particle two-phase turbulent flow in a vertical duct. *Int. J. Multiphase Flow* **21,** 1203–1228.

Chapman, S. and Cowling, T. G. (1970) *The Mathematical Theory of Non-uniform Gases*. Cambridge Mathematical Library, Cambridge.

Clift, R., Grace, J. R. and Weber, M. E. (1978) *Bubbles, Drops and Particles*. Academic Press, New York.

Csanady, G. T. (1963) Turbulent diffusion of heavy particles in the atmosphere. *J. Atm. Sci.* **105,** 329–334.

Dallavalle, J. M. (1948) *Micromeritics*. Pitman, London.

Delhaye, J. M. (1981) *Thermohydraulics of Two-phase Systems for Industrial Design and Nuclear Engineering*, ed. J. M. Delhaye.

Delhaye, J. M. (1974) Jump conditions and entropy sources in two-phase systems. Local formulation. *Int. J. Multiphase Flow* **1,** 395–409.

Delhaye, J. M. and Achard, J. L. (1977) On the use of averaging operators in two phase flow modeling. *Thermal and Hydraulic Aspects of Nuclear Reactor Safety, 1: Light Water Reactors*. ASME Winter Meeting.

Delhaye, J. M. and Achard, J. L. (1978) On the averaging operators introduced in two-phase flow. In *Transient Two-phase Flow*, ed. S. Banerjee and J. R. Weaver. Proc. CSNI Specialists Meeting, Toronto, 3–4 August.

Deutsch, E. and Simonin, O. (1991) Large eddy simulation applied to the motion of particles in stationary homogeneous turbulence. *Turbulence Modification in Multiphase Flow*, *ASME FED* **1,** 34–42.

Ding, J. and Gidaspow, D. (1990) A bubbling fluidization model using kinetic theory of granular flow. *AIChE Journal* **36,** 523–538.

Ding, J., Lyczkowski, R. W., Burge, S. W. and Gidaspow, D. (1992) Three-dimensional models of hydrodynamics and erosion in fluidized-bed combustors. *AIChE Symp. Ser.* **88,** 85–98.

Di Felice, R. (1994) The voidage function for fluid-particle interaction systems. *Int. J. Multiphase Flow* **20,** 153–159.

Drew, D. A. (1983) Mathematical modeling of two-phase flow. *Ann. Rev. Fluid Mech.* **15,** 261–291.
Drew, D. A. and Lahey, R. T. (1990) Some supplemental analysis concerning the virtual mass and lift force on a sphere in a rotating and straining flow. *Int. J. Multiphase Flow* **16,** 1127–1130.
Drew, D. A. and Lahey, R. T. (1993) In *Particulate Two-phase Flow*, Ch. 16, pp. 509–566, Butterworth-Heinemann, Boston.
Eilers, H. (1943) Die Viskositäts-Koncentrationsabhängigheit kolloider Systeme in organischen Lösungsmitteln. *Kolloid Zeitschrift* **102,** 154–169.
Einstein, A. (1906) Eine Neue Bestimmung der Molekuldimensionen. *Ann. Phys.* **19,** 289–306.
Einstein, A. (1911) Berichtigung zu meiner Arbeit: "Eine Neue Bestimmung der Molekuldimensionen". *Ann. Phys.* **34,** 591–592.
Elghobashi, S. E. and Abou-Arab, T. W. (1983) A two-equation turbulence model for two-phase flows. *Phys. Fluids* **26,** 931–938.
Enwald, H., Peirano, E., Almstedt, A. E. and Leckner, B. (1997) Simulation of the fluid dynamics of a bubbling fluidized bed: experimental validation of the two-fluid model and evaluation of a parallel multiblock solver. Submitted for publication.
Enwald, H. and Almstedt, A. E. (1997) Fluid dynamics of a pressurized fluidized bed: comparison between numerical solutions from two-fluid models and experimental results. In preparation.
Ergun, S. (1952) Fluid flow through packed columns. *Chem. Engng Progr.* **48,** 89–94.
Ettehadieh, B., Gidaspow, D. and Lyczkowski, R. W. (1984) Hydrodynamics of fluidization in a semicircular bed with a jet. *AIChE Journal* **30,** 529–536.
Foerster, S. F., Louge, M. Y., Chang, H. and Allia, K. (1994) Measurements of the collision properties of small spheres. *Phys. Fluids* **6,** 1108–1115.
Foscolo, P. U., Gibilaro, L. G. and Waldram, S. P. (1983) A unified model for particulate expansion of fluidized beds and flow in fixed porous media. *Chem. Engng Sci.* **38,** 1251–1260.
Frankel, N. A. and Acrivos, A. (1967) On the viscosity of a concentrated suspension of solid spheres. *Chem. Engng Sci.* **22,** 847–853.
Gatignol, R. (1983) The Faxén formulae for a rigid particle in an unsteady non-uniform Stokes flow. *Journal de Mécanique Théorique et Appliquée* **1,** 143–160.
Gibilaro, L. G., Di Felice, R. I. and Waldram, S. P. (1985) Generalized friction factor and drag coefficient correlations for fluid-particle interactions. *Chem. Engng Sci.* **40,** 1817–1823.
Gidaspow, D. (1986) Hydrodynamics of fluidization and heat transfer: supercomputer modelling. *Appl. Mech. Rev.* **39,** 1–22.
Gidaspow, D. (1994) *Multiphase Flow and Fluidization*. Academic Press, Boston.
Gidaspow, D. and Ettehadieh, B. (1983) Fluidization in two-dimensional beds with a jet II—Hydrodynamic modelling. *I & EC Fundam.* **22,** 193–201.
Gidaspow, D. and Syamlal, M. (1985) Solid–gas critical flow. *AIChE Meeting*, Chicago, 10–15 November.
Gidaspow, D., Shih, Y. T., Bouillard, J. and Wasan, D. (1989) Hydrodynamics of a lamella electrosettler. *AIChE Journal* **35,** 714–724.
Gidaspow, D. and Therdthianwong, A. (1993) Hydrodynamics and SO_2 absorption in a CFB loop. *AIChE Journal* **35,** 714–724.
Grad, H. (1949) On the kinetic theory of rarefied gases. *Comm. on Pure and Applied Mathematics* **2,** 331–407.
Graham, A. L. (1981) On the viscosity of suspensions of solid spheres. *Applied Scientific Research* **37,** 275–286.
He, J. and Simonin, O. (1994) Modélisation numérique des écoulements gaz-solides en conduite verticale. Rapport HE-44/94/021A, Laboratoire National d'Hydraulique, EDF, Chatou, France.
Hewitt, G. F. (1982) In *Handbook of Multiphase Systems*, ed. G. Hetsroni, Section 2.1, 2-3–2-43. McGraw-Hill, New York.
Hinze, J. O. (1975) *Turbulence*, 2nd edn. McGraw Hill, New York.
Hoomans, B. P. B., Kuipers, J. A. M., Briels, W. J. and Van Swaaij, W. P. M. (1996) Discrete particle simulation of bubble and slug formation in a two-dimensional gas-fluidized bed: a hard sphere approach. *Chem. Eng. Sci.* **51,** 99–108.
Hwang, G. J. and Shen, H. H. (1989) Modelling the solids phase stress in a fluid-solid mixture. *Int. J. Multiphase Flow* **15,** 257–268.

Ishii, M. (1975) *Thermo-fluid Dynamic Theory of Two-phase Flow*. Eyrolles, Paris.

Ishii, M. (1977) One-dimensional drift-flux model and constitutive equations for relative motion between phases in various two-phase flow regimes. Argonne National Laboratory Report, ANL-77-47.

Ishii, M. and Mishima, K. (1984) Two-fluid model and hydrodynamic constitutive relations. *Nuclear Engineering and Design* **82,** 107–126.

Ishii, M. and Zuber, N. (1979) Drag coefficient and relative velocity in bubbly, droplet or particulate flows. *AIChE J.* **25,** 843–855.

Jenkins, J. T. and Mancini, F. (1987) Balance laws and constitutive relations for plane flows for a dense, binary mixture of smooth, nearly elastic, circular disks. *J. Appl. Mech.* **54,** 27–34.

Jenkins, J. T. and Richman, M. W. (1985) Grad's 13 moment system for a dense gas of inelastic spheres. *Arch. Ratio. Mech. Anal.* **87,** 355–377.

Jenkins, J. T. and Savage, S. B. (1983) A theory for rapid flow of identical, smooth, nearly elastic, spherical particles. *J. Fluid. Mech.* **130,** 187–202.

Koch, D. L. (1990) Kinetic theory for a monodispersed gas–solid suspension. *Phys. Fluids A* **2,** 1711–1723.

Kuipiers, J. A. M., Prins, W. and van Swaaij, W. P. M. (1992a) Numerical calculation of wall-to-bed heat-transfer coefficients in gas-fluidized beds. *AIChE J.* **38,** 1079–1091.

Kuipiers, J. A. M., van Duin, K. J., van Beckum, F. P. H. and van Swaaij, W. P. M., (1992b) A numerical model of gas fluidized beds. *Chem. Engng Sci* **47,** 1913–1924.

Kuipiers, J. A. M., van Duin, K. J., van Beckum, F. P. H. and van Swaaij, W. P. M. (1993) Computer simulation of the hydrodynamics of a two-dimensional gas-fluidized bed. *Computers Chem. Engng* **17,** 839–858.

Kunii, D. and Levenspiel, O. (1991) *Fluidization Engineering*, 2nd edn. Butterworth-Heineman, Boston.

Lax, P. D. (1958) Differential equations, difference equations and matrix theory. *Comm. Pure Appl. Math.* **11,** 175–194.

Liang, L. and Michaelides, E. E. (1992) The magnitude of Basset forces in unsteady multiphase flow computations. *J. Fluid Eng.* **114,** 417–419.

Lun, C. K. K. (1991) Kinetic theory for granular flow of dense, slightly inelastic, slightly rough spheres. *J. Fluid Mech.* **233,** 539–559.

Lun, C. K. K. and Savage, S. B. (1986) The effects of an impact velocity dependent coefficient of restitution on stresses developed by sheared granular materials. *Acta Mechanica* **63,** 15–44.

Lyczkowski, R. W., Gidaspow, D., Solbrig, C. W. and Hughes, E. D. (1978) Characteristics and stability analyses of transient one-dimensional two-phase flow equations on their finite difference approximations. *Nuclear Sci. and Engng* **66,** 378–396.

Lyczkowski, R. W., Bouillard, J. X., Berry, G. F. and Gidaspow, D. (1987) Erosion calculations in a two-dimensional fluidized bed. *Proc. 9th Int. Conf. on FB Combustion* **2,** 697–706.

Lyczkowski, R. W., Folga, S., Chang, S. L., Bouillard, J. X., Wang, C. S., Berry, G. F. and Gidaspow, D. (1989) State of the art computation of dynamics and erosion in a fluidized bed tube banks. *Proc. 10th Int. Conf. on FB Combustion*, Vol. 1, pp. 465–477.

Lyczkowski, R. W., Gidaspow, D. and Solbrig, C. W. (1982) In *Advances in Transport Processes, Multiphase Flow—Models for Nuclear, Fossil and Biomass Energy Production*, ed. Mujumdar and Mashelker, pp. 198–351. Wiley, New York.

Lyczkowski, R. W., Gamwo, I. K., Dobran, F., Ai, Y. H., Chao, B. T. and Chen, M. M. (1991) Comparison of experimental and computed solids motion and bed dynamics for fluidized beds containing obstacles. *ASME FBC Conf.*, pp. 325–333.

Massoudi, M., Rajagopal, K. R., Ekmann, J. M. and Mathur M. P. (1992) Remarks on the modelling of fluidized systems. *AIChE J.* **38,** 471–472.

Maxey, M. R. and Riley, J. J. (1983) Equation of motion for a small rigid sphere in a nonuniform flow. *Phys. Fluids* **26,** 883–889.

O'Brien, T. J. and Syamlal, M. (1993) Particle cluster effects in the numerical simulation of a circulating fluidized bed. *4th Int. Conf. on CFB*, Somerset, USA, Preprint Volume, pp. 430–435.

Oesterlé, B. (1994) Une étude de l'influence des forces transversales agissant sur les particules dans les écoulements gaz–solide. *Powder Technology* **79,** 81–93.
Panton, R. L. (1984) *Incompressible Flow*. Wiley, New York.
Peirano, E. (1996) The Eulerian/Eulerian formulation applied to gas–particle flows. Report A96-218, Department of Energy Conversion, Chalmers University of Technology, Sweden.
Peirano, E., Palchonok, G., Johnsson, F. and Leckner, B. (1997) Estimates of turbulence mechanisms in circulating fluidized bed combustors. Submitted for publication.
Peirano, E. and Leckner, B. (1997) Fundamentals of turbulent gas–solid flows applied to circulating fluidized bed combustion. Submitted for publication.
Pritchett, J. W., Blake, T. R. and Garg, S. K. (1978) A numerical model of gas fluidized beds. *AIChE Symp. Ser.* **74,** 134–148.
Rashidi, M., Hetsroni, G. and Banergee, S. (1990) Particle-turbulence interaction in a boundary layer. *Int. J. Multiphase Flow* **16,** 935–949.
Rathmann, O. (1981) The added mass force, dependence on concentration by numerical solution. NORHAV-D-80, Risö National Laboratory, Denmark.
Reeks, M. W. (1992) On the continuum equations for dispersed particles in nonuniform flows. *Phys. Fluids A* **4,** 1290–1303.
Reeks, M. W. (1993) On the constitutive relations for dispersed particles in nonuniform flows. I. Dispersion in a simple shear flow. *Phys. Fluids A* **5,** 750–761.
Richardson, J. F. and Zaki, W. N. (1954) Sedimentation and fluidization. Part I. *Trans. Int. Chem. Engrs, London* **32,** 35–53.
Rivard, W. C. and Torrey, M. D. (1977) K-FIX: a computer program for transient, two dimensional, two fluid flow. LA-NUREG-6623, Los Alamos National Laboratory, Los Alamos.
Rizk, M. and Elghobashi, S. (1989) A two-equation turbulence model for dispersed dilute confined two-phase flows. *Int. J. Multiphase Flow* **15,** 119–133.
Roscoe, R. (1952) The viscosity of suspensions of rigid spheres. *Brit. J. Appl. Phys.* **3,** 267–269.
Rowe, P. N. (1971) In *Fluidization*, ed. J. F. Davidsson and D. Harrison, Ch. 4, pp. 187–188. Academic Press, London.
Savage, S. B. and Jeffrey, D. J. (1981) The stress tensor in a granular flow at high shear rates. *J. Fluid Mech.* **110,** 255–272.
Schiller, L. and Naumann, Z. (1935) *Z. Ver. Deutsch. Ing.* **77,** 318.
Simonin, O. (1990) Eulerain formulation for particle dispersion in turbulent two-phase flows. *Proc. 5th Workshop on Two-phase Flow Predictions*, Erlangen, FRG, pp. 156–166.
Simonin, O. (1995) Two-fluid model approach for turbulent reactive two-phase flows. Summer school on numerical modelling and prediction of dispersed two-phase flows, IMVU, Meserburg, Germany.
Simonin, O. and Viollet, P. L. (1989) Numerical study on phase dispersion mechanisms in turbulent bubbly flows. *Proc. 5th Workshop on Two-phase Flow Predictions*, Erlangen, FRG, pp. 156–166.
Soo, S. L. (1990) *Multiphase Fluid Dynamics*. Science Press, Gower Technical, New York.
Squire, K. D. and Eaton, J. K. (1994) Effect of selective modification of turbulence on two-equation models for particle-laden turbulent flows. *ASME J. Fluids Engng* **116,** 778–784.
Syamlal, M. and O'Brien, T. J. (1988) Simulation of granular layer inversion in liquid fluidized beds. *Int. J. Multiphase Flow* **14,** 473–481.
Syamlal, M. and O'Brien, T. J. (1989) Computer simulation of bubbles in a fluidized bed. *AIChE Symp. Ser.* **85,** 22–31.
Truesdell, C. and Toupin, R. (1960) In *Handbuch der Physik—Classical Field Theories*, pp. 700–704. Springer, Berlin.
Tsuo, Y. P. and Gidaspow, D. (1990) Computation of flow patterns in circulating fluidized beds. *AIChE Journal* **36,** 885–896.
Vand, V. (1948) Viscosity of solutions and suspensions. I—III. *J. Phy. Colloid Chem.* **52,** 277–321.
Vojir, D. J. and Michaelides, E. E. (1994) Effect of the history term on the motion of rigid spheres in a viscous fluid. *Int. J. Multiphase Flow* **20,** 547–556.
Wang, C. and Bouillard, J. X. (1993) Hydrodynamics/heat-transfer/erosion computer predictions for a cold small-scale CFBC. In *Circulating Fluidized Bed Technology IV*, pp. 359–366.
Wen, C. Y. and Yu, Y. H. (1966) Mechanics of fluidization. *AIChE Symp. Ser.* **62,** 100–111.

Whitaker, S. (1969) Advances in theory of fluid motion in porous media. *Ind. Eng. Chem.* **61,** 14–28.
Yonemura, T., Tanaka, T. and Tsuji, Y. (1995) Cluster formation in dispersed gas-solid flow (effect of physical properties of particles). *2nd Int. Conf on Multiphase Flow*, Kyoto, 3–7 April PT4 25–30.
Zuber, N. (1964) On the dispersed two-phase flow in the laminar flow regime. *Chem. Ind Sci.* **19,** 897–917.

APPENDIX A

Gauss' Theorem

Scalar function

$$\int_V \nabla f \, \mathrm{d}V = \int_A f\mathbf{n} \, \mathrm{d}A. \qquad [A1]$$

Vector function

$$\int_V \nabla\cdot\mathbf{f} \, \mathrm{d}V = \int_A \mathbf{f}\cdot\mathbf{n} \, \mathrm{d}A. \qquad [A2]$$

Tensor function

$$\int_V \nabla\cdot\bar{f} \, \mathrm{d}V = \int_A \bar{f}\cdot\mathbf{n} \, \mathrm{d}A. \qquad [A3]$$

Leibniz's Theorem

$$\frac{\mathrm{d}}{\mathrm{d}t}\int_{V_k(t)} f(\mathbf{r}, t)\mathrm{d}V = \int_{V_k(t)} \frac{\partial f}{\partial t}\,\mathrm{d}V + \int_{A_k(t)} f(\mathbf{u}_l\cdot\mathbf{n}_k)\mathrm{d}A. \qquad [A4]$$

APPENDIX B

Continuity Equation

Introducing the Reynolds-decomposed velocity vector of phase k into the averaged continuity equation [36], results in the following equation

$$\frac{\partial}{\partial t}\underbrace{(\langle X_k\rho_k\rangle)}_{\text{term 1}} + \underbrace{\nabla\cdot(\langle X_k\rho_k(\mathbf{U}_k+\mathbf{u}_k')\rangle)}_{\text{term 2}} = 0. \qquad [B1]$$

The transient term (term 1) is simplified using the phasic average of the density

$$\text{term 1} = \frac{\partial}{\partial t}(\alpha_k\rho_k^{X_k}). \qquad [B2]$$

In term 2, the mass-weighted average of the velocity vector is by definition constant on the scale of averaging. Utilizing this fact and the definitions given in section 3.4.2, the term can be rearranged in the following way

$$\text{term 2} = \nabla\cdot(\langle X_k\rho_k\rangle\mathbf{U}_k + \langle X_k\rho_k\mathbf{u}_k'\rangle)$$

$$= \nabla\cdot\left(\alpha_k\rho_k^{X_k}\left(\mathbf{U}_k + \underbrace{\langle\mathbf{u}_k'\rangle^{X_k\rho_k}}_{=0}\right)\right) = \nabla\cdot(\alpha_k\rho_k^{X_k}\mathbf{U}_k). \qquad [B3]$$

Thus, the Reynolds-decomposed and averaged continuity equations becomes

$$\frac{\partial}{\partial t}(\alpha_k\rho_k^{X_k}) + \nabla\cdot(\alpha_k\rho_k^{X_k}\mathbf{U}_k) = 0. \qquad [B4]$$

Momentum Equation

The Reynolds-decomposed velocity vector of phase k is first introduced into the ensemble-averaged momentum equation [37]

$$\underbrace{\frac{\partial}{\partial t}(\langle X_k\rho_k(\mathbf{U}_k+\mathbf{u}_k')\rangle)}_{\text{term 1}}+\underbrace{\nabla\cdot(\langle X_k\rho_k(\mathbf{U}_k+\mathbf{u}_k')(\mathbf{U}_k+\mathbf{u}_k')\rangle)}_{\text{term 2}}$$
$$\underbrace{-\nabla\cdot(\langle X_k\bar{\bar{T}}_k\rangle)}_{\text{term 3}}\underbrace{-\langle X_k\rho_k\mathbf{g}\rangle}_{\text{term 4}}=-\langle\bar{\bar{T}}_k\cdot\nabla X_k\rangle. \qquad [B5]$$

Starting with term 1, the expression inside the outer brackets is identical to that in the convective term of the continuity equation (term 2 in the continuity equation). In a way similar to the continuity equation, term 1 can thus be rewritten as

$$\text{term 1}=\frac{\partial}{\partial t}(\alpha_k\rho_k^{X_k}\mathbf{U}_k). \qquad [B6]$$

Term 2 is reformulated into the Reynolds-averaged form as follows

$$\begin{aligned}\text{term 2}&=\nabla\cdot(\langle X_k\rho_k\mathbf{U}_k\mathbf{U}_k\rangle+\langle 2X_k\rho_k\mathbf{U}_k\mathbf{u}_k'\rangle+\langle X_k\rho_k\mathbf{u}_k'\mathbf{u}_k'\rangle)\\&=\nabla\cdot\left(\langle X_k\rho_k\rangle\mathbf{U}_k\mathbf{U}_k+2\langle X_k\rho_k\rangle\mathbf{U}_k\underbrace{\langle\mathbf{u}_k'\rangle^{X_k\rho_k}}_{=0}-\alpha_k\bar{\bar{T}}_k^{\mathrm{Re}}\right) \qquad [B7]\\&=\nabla\cdot(\alpha_k\rho_k^{X_k}\mathbf{U}_k\mathbf{U}_k-\alpha_k\bar{\bar{T}}_k^{\mathrm{Re}}).\end{aligned}$$

Applying the phasic average to the stress and gravity terms, terms 3 and 4, respectively, the Reynolds-decomposed and averaged momentum equation is obtained as

$$\frac{\partial}{\partial t}(\alpha_k\rho_k^{X_k}\mathbf{U}_k)+\nabla\cdot(\alpha_k\rho_k^{X_k}\mathbf{U}_k\mathbf{U}_k)=\nabla\cdot(\alpha_k(\bar{\bar{T}}_k^{X_k}+\bar{\bar{T}}_k^{\mathrm{Re}}))+\alpha_k\rho_k^{X_k}\mathbf{g}+\mathbf{M}_{k\mathrm{I}}, \qquad [B8]$$

where $\mathbf{M}_{k\mathrm{I}}=-\langle\bar{\bar{T}}_k\cdot\nabla X_k\rangle$ is the interfacial momentum transfer term.